Article

Not peer-reviewed version

ESG Financial Market with Informed Traders within the Bachelier–Black–Scholes–Merton Model

Nancy Asare Nyarko *, Bhathiya Divelgama, Peter Yegon, Brent Lindquist, Svetlozar Rachev, Abootaleb Shirvani, Frank Fabozzi

Posted Date: 6 February 2025

doi: 10.20944/preprints202502.0372.v1

Keywords: ESG finance; Bachelier's model; Black–Scholes–Merton model; option prices; binomial pricing trees

 doi:10.20944/preprints202502.0372.v1

Article

ESG Financial Market with Informed Traders within the Bachelier–Black–Scholes–Merton Model

Nancy Asare Nyarko [1,*], Bhathiya Divelgama [1], Peter Yegon [1], W. Brent Lindquist [1], Svetlozar T. Rachev [1], Abootaleb Shirvani [2] and Frank J. Fabozzi [3]

[1] Department of Mathematics & Statistics, Texas Tech University, Lubbock, TX, USA
[2] Department of Mathematical Science, Kean University, Union, NJ, USA
[3] Carey Business School, Johns Hopkins University, Baltimore, MD, USA
* Correspondence: nasareny@ttu.edu

Abstract: This study seeks to advance the theory of dynamic asset pricing by introducing asset valuation, adjusted by environmental, social and governance (ESG) ratings, within a unified Bachelier–Black–Scholes–Merton market model, and developing option valuation in both continuous-time and discrete-time (binomial pricing tree) frameworks. An empirical study based on call option prices for assets selected from the Nasdaq-100 develops implied values for the main ESG parameter in the pricing model. For these stocks, option traders have in-the-money ESG valuations that are lower than the spot price. Within the discrete-time framework, we demonstrate how an informed trader can adopt a futures trading strategy to optimize an effective dividend stream.

Keywords: ESG finance; Bachelier's model; Black–Scholes–Merton model; option prices; binomial pricing trees

1. Introduction

Despite initial rejection of the Bachelier model (Bachelier 1900), its arithmetic Brownian motion dynamics have found acceptance in certain areas. To combine the strengths of both arithmetic and geometric Brownian motion models, the classical Black–Scholes–Merton (BSM) model (Black and Scholes 1973; Merton 1973) has been merged with a modernized Bachelier (MB) model (Rachev et al. 2024), producing a unified Bachelier–Black–Scholes–Merton (BBSM) model (Lindquist et al. 2024). Both the unified model and its MB limit allow for price trajectories taking values in $\mathbb{R}$, while, under the BSM limit, price processes take values in $\mathbb{R}^+$. Exploiting the more extensive price range of the MB model, Rachev et al. (2024) developed a dynamic ESG-adjusted valuation ("ESG-adjusted pricing") for assets, which allows for stocks with low ESG ratings to be given a negative ESG-adjusted value. A critical parameter of the adjusted valuation is the so-called ESG affinity, quantifying the market view of the "size" of the contribution of ESG ratings to asset values. Asare Nyarko et al. (2023) explored fair valuation of options under the MB model using this ESG-adjusted asset valuation.

Consideration of ESG factors in financial modeling marks a paradigm shift in how asset values are assessed. As the world evolves toward a greener future, industry leaders must champion sustainability. (However, see Del Mar Miralles-Quiros et al. (2017) for a study of how sustainability efforts have varied by market). Providing a solid quantitative use for ESG ratings is an important step in the effort to champion sustainability in the financial world. Consideration of ESG-adjusted prices alters the investment approach required for long-term investing, enabling ESG-conscious investors to more effectively measure, and (potentially) profit from, ESG strategies. Analyses based on such pricing must be woven into the investment processes of any discerning investor, as well as integrated into the corporate strategy of any company that is truly committed to increasing shareholder value (Fulton et al. 2012).

The first goal of this paper is to embed ESG asset valuation within the continuous-time BBSM model (Section 2), placing ESG finance within the broader framework of a unified Bachelier and

 doi:10.20944/preprints202502.0372.v1

Black–Scholes–Merton theory. In Section 3, we embed the ESG-adjusted asset valuation into the BBSM binomial option pricing model of Lindquist et al. (2024).

The second goal is to provide an empirical study of discrete option pricing under the ESG-BBSM binomial model of Section 3. Our data set for 16 stocks selected from the Nasdaq-100 is described in Section 4.1. Empirical examples of ESG-adjusted prices are presented in Section 4.2. In Section 4.3 we describe how to fit the required parameters of the binomial model to empirical data. In Section 5, using published call option prices for 01/02/2024, we compute implied values of the ESG affinity parameter as functions of strike price and time to maturity. These can then be expressed in terms of an implied ESG valuation (as a function of strike price and time to maturity). Comparing the implied ESG valuation to financial spot prices provides insight into the views of option traders on the impact of ESG ratings on the underlying asset value.

The third goal of this study (Section 6) focuses on a discrete-time, futures trading strategy that can be adopted by an option hedger (the trader taking a short position on an option) who may posses information regarding the future direction of movement of the ESG-adjusted valuation of the underlying stock. While the efficient market hypothesis argues that the direction of the asset price movement is unpredictable (Alexander 1961, 1964; Cootner 1964; Fama 1965, 1970, 1991, 1995; Jensen 1978; Osborne 1959), numerous studies challenge this view and indicate that price direction may, indeed, be predictable (Abu-Mostafa and Atiya 1996; Ang et al. 2010; Campbell and Thomson 2008; Cervelló-Royo et al. 2015; Chong et al. 2017; Chung and Hong 2014; Leung et al. 2000; Malkiel 2003; Naseer and Yasir 2014; Qiu and Song 2016; Rubén et al. 2017; Shah et al. 2019; Shiller 2003; Zhong and Enke 2017, 2019). As a result, Chakravarty et al. (2004); Collin-Dufresne et al. (2021); Turkington and Walsh (2000) and many others have worked on understanding informed trading markets and the strategies employed. We demonstrate that the trader can optimize this trading strategy to produce an effective dividend stream.

Section 7 concludes the paper with a discussion of future directions.

2. Embedding ESG pricing in the BBSM model

Consider the market $(\mathcal{A}, \mathcal{B}, \mathcal{C})$ consisting of a risky asset $\mathcal{A}$, a riskless asset $\mathcal{B}$, and a European contingency claim (option) $\mathcal{C}$. Under BBSM, $\mathcal{A}$ has the price dynamics of a continuous diffusion process determined by the stochastic differential equation

$$\begin{aligned} &dA_t = \varphi(A_t,t)dt + \psi(A_t,t)dB_t\,, \quad t \geq 0\,, \quad A_0 > 0, \\ &\varphi(A_t,t) = a_t + \mu_t A_t, \qquad \psi(A_t,t) = v_t + \sigma_t A_t, \end{aligned} \tag{1}$$

where $B_t \in [0,\infty)$ is a standard Brownian motion on a stochastic basis

$$(\Omega, \mathcal{F}, \mathbb{F} = \{\mathcal{F}_t = \sigma(B_u, u \leq t) \subseteq \mathcal{F}, t \geq 0\}, \mathbb{P})$$

of a complete probability space $(\Omega, \mathcal{F}, \mathbb{P})$. The coefficients satisfy $a_t \in \mathbb{R}$, $\mu_t \in \mathbb{R}$, $v_t \geq 0$, $\sigma_t \geq 0$, and are $\mathcal{F}$-adapted processes. The $\mathcal{F}$-adapted processes $\varphi(A_t,t)$ and $\psi(A_t,t)$ are assumed to satisfy the usual regularity conditions.[1] Lindquist et al. (2024) define the appropriate price dynamics[2] of the riskless asset $\mathcal{B}$ in the BBSM market model as

$$d\beta_t = \chi(\beta_t,t)dt, \quad \chi(\beta_t,t) = \rho_t + r_t\beta_t, \quad t \geq 0, \quad \beta_0 > 0. \tag{2}$$

[1] The regularity conditions require that $\varphi(x,t)$ and $\psi(x,t)$ satisfy the Lipschitz and growth conditions in $x \in \mathbb{R}$ for $t \geq 0$ (Duffie 2001, Section 5G and Appendix E). We also require $\int_0^t |\varphi(x,s)|\,ds < \infty$ and $\int_0^t |\psi(x,s)^2|\,ds < \infty$ for all $t \geq 0$ and $x \in \mathbb{R}$. To simplify the exposition, we will assume that a_t, μ_t, v_t, and σ_t have trajectories that are continuous and uniformly bounded on $t \in [0,\infty)$.

[2] Any other choice will result in a riskless asset whose dynamics are inconsistent with that of the risky asset.

 doi:10.20944/preprints202502.0372.v1

Again, $\rho_t \in \mathbb{R}$ and $r_t \in \mathbb{R}$ are $\mathcal{F}$-adapted processes. The $\mathcal{F}$-adapted process $\chi(\beta_t, t)$ is also assumed to satisfy the usual regularity conditions.[3] The MB model is achieved as the limiting case $\mu_t = \sigma_t = r_t = 0$, while the classical BSM model is the limiting case $a_t = v_t = \rho_t = 0$. For brevity, we adopt the notation $\varphi_t = \varphi(A_t, t)$, $\psi_t = \psi(A_t, t)$ and $\chi_t = \chi(\beta_t, t)$. We require $\psi_t > 0$, $\mathbb{P}$-almost surely (a.s.). A necessary condition for no-arbitrage is the requirement that $\beta_t \leq A_t$, $\mathbb{P}$-a.s. Under the no-arbitrage assumption, the market price of risk is

$$\Theta_t = \frac{\varphi_t - \chi_t}{\psi_t}, \tag{3}$$

which is strictly positive $\mathbb{P}$-a.s. for all $t \geq 0$ providing $\varphi_t > \chi_t$, $\mathbb{P}$-.a.s.

The option $\mathcal{C}$ has the price dynamics

$$C_t = f(A_t, t), \quad t \in [0, T], \tag{4}$$

where $f(x, t)$, $x \in \mathbb{R}$, $t \in [0, T]$, has continuous partial derivatives $\partial^2 f(x,t)/\partial x^2$ and $\partial f(x,t)/\partial t$ on $t \in [0, T)$, and T is the expiration (maturity) time of $\mathcal{C}$. The option's maturity payoff is $C_T = g(A_T)$ for some continuous function $g : \mathbb{R} \to \mathbb{R}$. The risk-neutral valuation of C_t is (Lindquist et al. 2024)

$$C_t = \mathbb{E}_t^{\mathbb{Q}}\left[\exp\left(-\int_t^T \left(r_u + \frac{\rho_u}{\beta_u}\right) du\right) g(A_T)\right], \quad t \in [0, T], \tag{5}$$

where $\mathbb{Q} \equiv \mathbb{P}$ is the equivalent martingale measure and the asset price dynamics under $\mathbb{Q}$ is

$$dA_t = \left(r_t + \frac{\rho_t}{\beta_t}\right) A_t dt + \psi_t dB^{\mathbb{Q}}(t), \quad t \geq 0. \tag{6}$$

In (6), $B_t^{\mathbb{Q}}$, $t \in [0, \infty)$, is a standard Brownian motion on the stochastic basis $(\Omega, \mathcal{F}, \mathbb{F}, \mathbb{Q})$.

Consider a published ESG rating[4] (score) $Z_t^{(X)} \in [0, 10]$ for a company X at time t. Rachev et al. argue that bounded scales for an ESG score do not differentiate adequately between the amount of effort that a company must undergo to raise their score above a current value.[5] They further argue that scores based upon a convex, monotonically increasing function better represent such effort, and that the choice of such a function should be based ultimately on an axiomatic approach. In the absence of such an approach, they proposed the relative ESG measure

$$Z_t^{(X;I)} = \frac{Z_t^{(X)} - Z_t^{(I)}}{Z_t^{(I)}}, \tag{7}$$

where $Z_t^{(X)}$ is the ESG rating (score) of company X and $Z_t^{(I)}$ is the ESG score of a relevant market index I.[6] They further define the ESG-adjusted stock price of company X at time $t \geq 0$ by

$$A_t = S_t^{(X)}(1 + \gamma Z_t^{(X;I)}), \tag{8}$$

---

[3] The regularity conditions require that $\chi(x, t)_t$ satisfies the Lipschitz and growth conditions in $x \in \mathbb{R}$ for $t \geq 0$. We also require $\int_0^t |\chi(x, s)|\, ds < \infty$ for all $t \geq 0$ and $x \in \mathbb{R}$. To simplify the exposition, we will assume that ρ_t and r_t have trajectories that are continuous and uniformly bounded on $t \in [0, \infty)$.

[4] Typically the scores $Z_t^{(X)}$ are on a zero-to-ten or a zero-to-one-hundred scale. Our data provider, Bloomberg Professional Services, uses the zero-to-ten scale.

[5] The amount of effort to raise an ESG score from 0 to 0.5 is trivial compared to the effort required to raise a score from 9.5 to 10.0.

[6] Under (7), the value of $Z_t^{(X;I)}$ is independent of the range of the scale as long as the range is finite and the same range is used for both $Z_t^{(X)}$ and $Z_t^{(I)}$.

 doi:10.20944/preprints202502.0372.v1

which incorporates ESG scores as part of an asset's valuation. Here $S_t^{(X)} > 0$ represents the financial price of an asset, while $A_t \in \mathbb{R}$ represents an ESG-adjusted valuation,[7] which Rachev et al. refer to as the ESG-adjusted price. In (8), $\gamma \in \mathbb{R}$ is referred to as the ESG affinity of the financial market.[8]

The ESG-adjusted stock price (8) can be negative.[9] This is not surprising as the relative score $Z_t^{(X;I)}$ is analogous to any financial 'spread'. We note the following dependencies of A_t on γ.

$$A_t = S_t^{(X)} + \gamma\left(S_t^{(X)} Z_t^{(X;I)}\right), \tag{9a}$$

$$A_{t+1} - A_t = S_{t+1}^{(X)} - S_t^{(X)} + \gamma\left(S_{t+1}^{(X)} Z_{t+1}^{(X;I)} - S_t^{(X)} Z_t^{(X;I)}\right). \tag{9b}$$

$$\mathbb{E}[A_t] = \mathbb{E}\left[S_t^{(X)}\right] + \gamma\mathbb{E}\left[S_t^{(X)} Z_t^{(X;I)}\right], \tag{9c}$$

$$\mathrm{Var}[A_t] = \mathrm{Var}\left[S_t^{(X)}\right] + 2\gamma\mathrm{Cov}\left[S_t^{(X)}, S_t^{(X)} Z_t^{(X;I)}\right] + (\gamma)^2\mathrm{Var}\left[S_t^{(X)} Z_t^{(X;I)}\right], \tag{9d}$$

From (9a) through (9d), we see that changing the value of γ only affects the (additional) fractional financial price term $Z_t^{(X;I)} S_t^{(X)}$, which satisfies $|Z_t^{(X;I)} S_t^{(X)}| \leq S_t^{(X)}$.

3. Binomial Option Pricing under the BBSM Model

Lindquist et al. (2024, Section 7) developed a binomial option pricing model under the BBSM model. We briefly summarize that model here. Consider a BBSM market $(\mathcal{A}, \mathcal{B}, \mathcal{C})$ consisting of the risky asset (stock) $\mathcal{A}$, the $\mathcal{B}$ and call option $\mathcal{C}$. The stock price A_t evolves according to the binomial pricing tree

$$A_{(k+1)\Delta,n} = \begin{cases} A^{(u)}_{(k+1)\Delta,n} = A_{k\Delta,n} + u_{k\Delta,n}, & \text{if} \quad \zeta_{k+1,n} = 1, \\ A^{(d)}_{(k+1)\Delta,n} = A_{k\Delta,n} + d_{k\Delta,n}, & \text{if} \quad \zeta_{k+1,n} = 0. \end{cases} \tag{10}$$

In (10), $A_{k\Delta,n}$, $k = 0, 1, \ldots, n$, $n \in \mathbb{N} = \{1, 2, \ldots\}$, is the stock price at time $k\Delta$, $\Delta = \Delta_n = T/n$ where T is the fixed maturity time and $A_0 > 0$. For every $n \in \mathbb{N}$, $\zeta_{k,n}$, $k = 1, 2, \ldots, n$, are independent, identically distributed Bernoulli random variables with $P(\zeta_{k,n} = 1) = 1 - P(\zeta_{k,n} = 0) = p_n$ determining the filtration

$$\mathbb{F}^{(n)} = \left\{\mathcal{F}_k^{(n)} = \sigma(\zeta_{j,n} : j = 1, \ldots, k),\ \mathcal{F}_0^{(n)} = \{\emptyset, \Omega\},\ \zeta_{0,n} = 0\right\} \tag{11}$$

of the stochastic basis $(\Omega, \mathcal{F}, \mathbb{F}^{(n)}, P)$ on the complete probability space $(\Omega, \mathcal{F}, \mathbb{P})$. The riskless asset $\mathcal{B}$ has the discrete price dynamics

$$\beta_{(k+1)\Delta,n} = \beta_{k\Delta,n} + \chi_{k\Delta,n}\Delta, \quad k = 0, 1, \ldots, n-1, \quad \beta_{0,n} > 0. \tag{12}$$

where $\chi_{k\Delta,n}$ is the instantaneous rate of (2) at times $k\Delta$.

Under BBSM, price changes, rather than returns, are of primary interest. Let

$$c_{(k+1)\Delta,n} = A_{(k+1)\Delta,n} - A_{k\Delta,n}, \quad k = 0, \ldots, n-1, \quad c_{0,n} = 0. \tag{13}$$

Then,

$$c_{(k+1)\Delta,n} = \begin{cases} c^{(u)}_{(k+1)\Delta,n} = u_{k\Delta,n}, & \text{w.p.} \quad p_n, \\ c^{(d)}_{(k+1)\Delta,n} = d_{k\Delta,n}, & \text{w.p} \quad 1 - p_n. \end{cases} \tag{14}$$

[7] In our view, the relative ESG score (which like return and risk-measure is dimensionless), adds a third dimension to conventional risk – return analyses of dynamic asset prices.

[8] As noted in Rachev et al. (2024, footnote 6), the ESG affinity is expected to change slowly with time. Here we assume it is constant over the both the historical window of prices and the option price maturity times considered.

[9] Hence Rachev et al. (2024) argued that the MB model, rather than BSM, is better designed to capture the trajectories of ESG-adjusted prices.

 doi:10.20944/preprints202502.0372.v1

In order that the càdlàg process on the Skorokhod space $D[0,T]$ generated by the binomial tree (10) converge weakly to the continuous time process (1), we require that the conditional mean and variance satisfy

$$\mathbb{E}[c_{(k+1)\Delta,n}|\mathcal{F}_k^{(n)}] = \varphi_{k\Delta,n}\Delta, \quad \mathrm{Var}[c_{(k+1)\Delta,n}|\mathcal{F}_k^{(n)}] = \psi^2_{k\Delta,n}\Delta, \tag{15}$$

where $\varphi_{k\Delta,n}$ and $\psi^2_{k\Delta,n}$ are the instantaneous mean and variance of (6) at time $k\Delta$. Then $u_{k\Delta,n}$ and $d_{k\Delta,n}$ are given by

$$u_{k\Delta,n} = \varphi_{k\Delta,n}\Delta + \sqrt{\frac{1-p_n}{p_n}}\psi_{k\Delta,n}\sqrt{\Delta}\,, \qquad d_{k\Delta,n} = \varphi_{k\Delta,n}\Delta - \sqrt{\frac{p_n}{1-p_n}}\psi_{k\Delta,n}\sqrt{\Delta}\,. \tag{16}$$

The option $\mathcal{C}$ has the discrete price dynamics $C_{k\Delta,n} = C(A_{k\Delta,n}, k\Delta)$, $k = 0,\ldots,n-1$. Consider a self-financing strategy, $P_{k\Delta,n} = \eth_{k\Delta,n}A_{k\Delta,n} + {}_{k\Delta,n}\beta_{k\Delta,n}$ replicating the option price process $C_{k\Delta,n}$:

$$\begin{aligned}
\eth_{k\Delta,n}A_{k\Delta,n} + {}_{k\Delta,n}\beta_{k\Delta,n} &= C_{k\Delta,n},\\
\eth_{k\Delta,n}A^{(u)}_{(k+1)\Delta,n} + {}_{k\Delta,n}\beta_{(k+1)\Delta,n} &= C^{(u)}_{(k+1)\Delta,n},\\
\eth_{k\Delta,n}A^{(d)}_{(k+1)\Delta,n} + {}_{k\Delta,n}\beta_{(k+1)\Delta,n} &= C^{(d)}_{(k+1)\Delta,n}.
\end{aligned}$$

The standard no-arbitrage arguments lead to

$$\begin{aligned}
\eth_{k\Delta,n} &= \frac{C^{(u)}_{(k+1)\Delta,n} - C^{(d)}_{(k+1)\Delta,n}}{u_{k\Delta,n} - d_{k\Delta,n}},\\
{}_{k\Delta,n} &= \frac{1}{\beta_{k\Delta,n} + \chi_{k\Delta,n}\Delta}\left(C^{(u)}_{(k+1)\Delta,n} - \frac{C^{(u)}_{(k+1)\Delta,n} - C^{(d)}_{(k+1)\Delta,n}}{u_{k\Delta,n} - d_{k\Delta,n}}A^{(u)}_{(k+1)\Delta,n}\right).
\end{aligned} \tag{17}$$

Thus, the risk-neutral valuation of the option is given by the recursion

$$C_{k\Delta,n} = \frac{\beta_{k\Delta,n}}{\beta_{k\Delta,n} + \chi_{k\Delta,n}\Delta}\Big(q_{k\Delta,n}C^{(u)}_{(k+1)\Delta,n} + (1-q_{k\Delta,n})C^{(d)}_{(k+1)\Delta,n}\Big), \tag{18}$$

where the risk-neutral probability $q_{k\Delta,n}$ is

$$q_{k\Delta,n} = p_n - \frac{\varphi_{k\Delta,n} - \frac{\chi_{k\Delta,n}}{\beta_{k\Delta,n}}A_{k\Delta,n}}{\psi_{k\Delta,n}}\sqrt{p_n(1-p_n)\Delta}\,. \tag{19}$$

The limit $a_{k\Delta,n} = v_{k\Delta,n} = \rho_{k\Delta,n} = 0$ of (18) and (19) produces the option price recursion relation for the BSM model,

$$C_{k\Delta,n} = \frac{1}{1 + r_{k\Delta,n}\Delta}\Big(q_{k\Delta,n}C^{(u)}_{(k+1)\Delta,n} + (1-q_{k\Delta,n})C^{(d)}_{(k+1)\Delta,n}\Big), \tag{20}$$

having risk-neutral probability

$$q_{k\Delta,n} = p_n - \theta_{k\Delta,n}\sqrt{p_n(1-p_n)\Delta}\,, \tag{21}$$

where $\theta_{k\Delta,n}$ is the discrete form of the market price of risk, $\theta_t = (\mu_t - r_t)/\sigma_t$, $t \geq 0$, in the BSM model.[10] In this limit, the discrete price of the riskless asset obeys, $\beta_{k\Delta,n} = \beta_0\prod_{j=0}^{k-1}(1 + r_{j\Delta,n}\Delta)$.

[10] In agreement with Hu et al. (2020).

 doi:10.20944/preprints202502.0372.v1

The limit $\mu_{k\Delta,n} = \sigma_{k\Delta,n} = r_{k\Delta,n} = 0$, produces the option price recursion relation for the Rachev et al. (2024) Bachelier model,

$$C_{k\Delta,n} = \frac{\beta_{k\Delta,n}}{\rho_{k\Delta,n} + \beta_{k\Delta,n}} \left(q_{k\Delta,n} C^{(u)}_{(k+1)\Delta,n} + (1 - q_{k\Delta,n}) C^{(d)}_{(k+1)\Delta,n} \right). \tag{22}$$

The risk-neutral probability $q_{k\Delta,n}$ is (see also Hu et al. 2020),

$$q_{k\Delta,n} = p_n - \frac{a_{k\Delta,n} - \frac{\rho_{k\Delta,n}}{\beta_{k\Delta,n}} A_{k\Delta,n}}{v_{k\Delta,n}} \sqrt{p_n(1-p_n)\Delta}\,. \tag{23}$$

In this limit, the discrete price of the riskless asset obeys $\beta_{k\Delta,n} = \beta_0 + \sum_{j=0}^{k-1} \rho_{j\Delta,n}\Delta$.

3.1. The Binomial Model is Not Recombining

A careful analysis shows that the risky-asset asset price process (10) does not, in fact, form a recombining tree. For a fixed value of k, $k = 0, 1, ..., n$, the superscripts (u) and (d) determine node "level" values at time $k+1$. For a recombining binomial tree, at time k, there are $k+1$ level numbers Thus each node on the tree is indexed by a k, j pair, $k = 0, ..., n$, $j = 1, ..., k+1$. With the inclusion of level numbers, (10) is written as

$$\begin{aligned} A^{j+1}_{(k+1)\Delta,n} &= A^{j}_{k\Delta,n} + u^{j}_{k\Delta,n}, \quad \text{w.p. } p, \\ A^{j}_{(k+1)\Delta,n} &= A^{j}_{k\Delta,n} + d^{j}_{k\Delta,n}, \quad \text{w.p. } 1-p, \end{aligned} \tag{24}$$

where, from (16),

$$\begin{aligned} u^{j}_{k\Delta,n} &= \varphi^{j}_{k\Delta,n}\Delta + p^{(u)}\psi^{j}_{k\Delta,n}\sqrt{\Delta}, & d^{j}_{k\Delta,n} &= \varphi^{j}_{k\Delta,n}\Delta - p^{(d)}\psi^{j}_{k\Delta,n}\sqrt{\Delta}, \\ \varphi^{j}_{k\Delta,n} &= a + \mu A^{j}_{k\Delta,n}, & \psi_{k\Delta,n} &= v + \sigma A^{j}_{k\Delta,n}, \\ p^{(u)} &= \sqrt{\frac{1-p_n}{p_n}}, & p^{(d)} &= \sqrt{\frac{p_n}{1-p_n}}. \end{aligned} \tag{25}$$

Fig. 1 illustrates a price configuration on four nodes of the tree, with time and level values indicated.

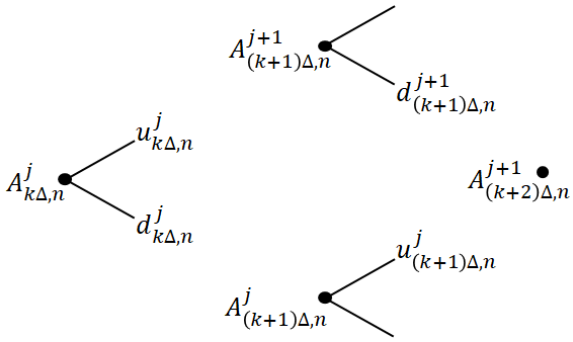

Figure 1. Time and level notation for the price evolution of the risky asset on the BBSM binomial tree.

Substituting (25) into (24) gives

$$\begin{aligned} A^{j+1}_{(k+1)\Delta,n} &= \alpha^{+} A^{j}_{k\Delta,n} + \eta^{+}, \quad \text{w.p. } p, \\ A^{j}_{(k+1)\Delta,n} &= \alpha^{-} A^{j}_{k\Delta,n} + \eta^{-}, \quad \text{w.p. } 1-p, \end{aligned} \tag{26}$$

where

$$\begin{aligned} \alpha^{+} &= 1 + \mu\Delta + p^{(u)}\sigma\sqrt{\Delta}, & \eta^{+} &= a\Delta + p^{(u)}v\sqrt{\Delta}, \\ \alpha^{-} &= 1 + \mu\Delta - p^{(d)}\sigma\sqrt{\Delta}, & \eta^{-} &= a\Delta - p^{(d)}v\sqrt{\Delta}. \end{aligned} \tag{27}$$

 doi:10.20944/preprints202502.0372.v1

Table 1. Summaries of the 16 stocks used in the empirical study.

Ticker	Company Name	GICS Sector	Headquarters
AAPL	Apple Inc.	information technology	Cupertino, CA
AMAT	Applied Materials, Inc.	information technology	Santa Clara, CA
AMD	Advanced Micro Devices, Inc.	information technology	Santa Clara, CA
AMZN	Amazon.com, Inc.	consumer discretionary	Bellevue, WA
ASML	ASML Holding NV	information technology	Veldhoven, NL
CSX	CSX Corp.	industrials	Jacksonville, FL
DLTR	Dollar Tree, Inc.	consumer discretionary	Chesapeake, VA
EA	Electronic Arts, Inc.	communication services	Redwood City, CA
GOOGL	Alphabet, Inc.	communication services	Mountain View, CA
INTC	Intel Corp.	information technology	Santa Clara, CA
NVDA	Nvidia Corp.	information technology	Santa Clara, CA
PANW	Palo Alto Networks, Inc.	information technology	Santa Clara, CA
ROST	Ross Stores, Inc.	consumer discretionary	Dublin, CA
TEAM	Atlassian Corp.	information technology	Sydney, AU
WDAY	Workday, Inc.	information technology	Pleasanton, CA
WBD	Warner Bros Discovery, Inc.	communication services	New York, NY

Note that α^+, α^-, η^+, and η^- are constants.

For the tree to be recombining, in Fig. 1 we must have

$$A^{j+1}_{(k+2)\Delta,n} = \alpha^+ A^{j}_{(k+1)\Delta,n} + \eta^+ = \alpha^- A^{j+1}_{(k+1)\Delta,n} + \eta^- . \tag{28}$$

With some algebra, the difference

$$\epsilon = \left(\alpha^+ A^{j}_{(k+1)\Delta,n} + \eta^+\right) - \left(\alpha^- A^{j+1}_{(k+1)\Delta,n} + \eta^-\right)$$

can be shown to be

$$\epsilon = \frac{a\sigma - v\mu}{\sqrt{p_n(1-p_n)}}\Delta^{3/2}, \tag{29}$$

independent of time or level number.[11] To ensure that the tree is numerically recombining in our empirical work in Section 4, we define

$$A^{j+1}_{(k+2)\Delta,n} = 0.5\left(\alpha^+ A^{j}_{(k+1)\Delta,n} + \eta^+ + \alpha^- A^{j+1}_{(k+1)\Delta,n} + \eta^-\right). \tag{30}$$

We note that ϵ vanishes more rapidly than $\sqrt{\Delta}$ and Δ terms as $\Delta \downarrow 0$. However, theoretical work remains to be done to ascertain whether the càdlàg process on the Skorokhod space $D[0,T]$ generated by either (10) or (30) does indeed converge weakly to the continuous time process (1). We leave this question open for further investigation. We do note that the BSM and MB limits of the price process (10) are indeed recombining (binomial) trees whose generated càdlàg processes do converge weakly to the appropriate BSM and MB limits of the continuous time process (1).

4. Empirical Examples: ESG-adjusted Prices and Parameter Fitting

4.1. The Data

Table 1 provides brief summaries of the 16 companies in the Nasdaq-100 index () as of 01/02/2024 that we considered for our empirical study.[12] Adjusted closing prices for the period 01/04/2016

[11] None-the-less, these constant errors propagate multiplicatively along the tree.

[12] The stocks were chosen to represent the full range of ESG scores.

 doi:10.20944/preprints202502.0372.v1

through 01/02/2024 were obtained for these stocks from Yahoo Finance.[13] ESG scores for all 101 asset class shares in were obtained from Bloomberg Professional Services.[13] Bloomberg provides "fiscal year" ESG scores.[14] On 01/02/2024, yearly ESG scores were available for FY 2015 through FY 2022; scores for FY 2023 had not yet been released. Therefore the ESG scores for FY2023 were set equal to those for FY2022. Individual stock weights for the ETF Invesco QQQ Trust, Series 1 were used as proxies for actual weights.[15] In our view this is a preferable choice for the weights as the ETF is a tradeable instrument that is designed to track the .

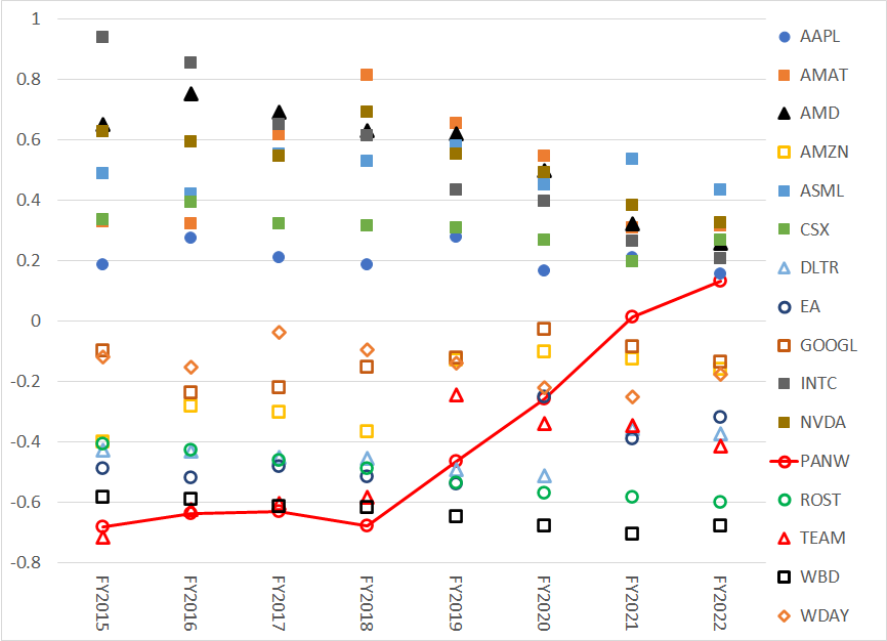

Figure 2 The relative ESG scores $Z_t^{(X;)}$ of the 16 chosen companies.

Using the QQQ weights, a weighted ESG score for was computed for each fiscal year. Fig. 2 shows the resultant fiscal year, relative ESG scores $Z_t^{(X;)}$ of the 16 chosen companies. Seven of the stocks have positive relative ESG scores over the entire 8 years of data; eight have negative relative ESG scores; and only one, PANW, has an ESG score that increases from below the index value to above. We note that, with the exception of PANW, the change in the ESG score of most companies relative to the index weighted average has remained approximately constant, or decreased, since 2019.

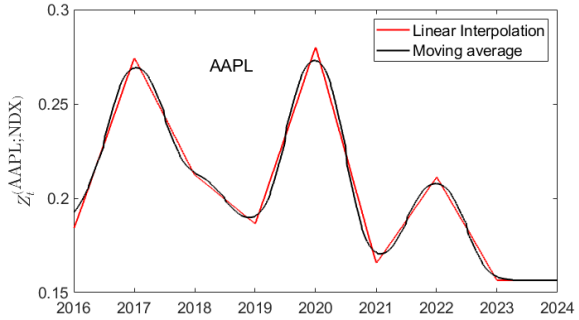

Figure 3 Illustration of the two-step smoothing process for $Z_t^{(AAPL;)}$.

[13] Accessed 01/02/2024.

[14] "Fiscal year scores are provided for a given company once complete ESG data for a specific fiscal year is published." Source: Bloomberg ESG Scores: Overview & FAQ. https://hr.bloombergadria.com/data/files/Pitanja%20i%20odgovori%20o%20Bloomberg%20ESG%20Scoreu.pdf Accessed 12/22/2024.

[15] Source https://www.slickcharts.com/nasdaq100. Accessed 01/02/2024.

 doi:10.20944/preprints202502.0372.v1

The ESG data were smoothed to provide daily values. Specifically we smoothed the values of $Z_t^{(X;)}$. The fiscal year values were assigned to the last day (December 31) of the year (with the ESG score for 01/02/2024 being set equal to the 12/31/2022 value). The daily smoothing, which consisted of two steps: linear interpolation followed by a Gaussian-weighted, moving average smoothing function, provided daily values between 12/31/2015 and 01/02/2024. The linear interpolation produced daily values between successive year end values. The Gaussian-weighted, moving average produced a smoother $Z_t^{(X;)}$ curve having the property that it produces no data "overshoot" or "undershoot". Fig. 3 shows an example of the smoothing for $Z_t^{(\text{AAPL;})}$.

4.2. ESG-Adjusted Prices

In Section 5, implied values for γ were estimated from call option prices, reflecting the view of option traders. However, there is no estimate for values of γ based upon historical spot trading. In order to investigate historical ESG-adjusted prices, we proceeded as follows. We assumed that the financial price series $S_t^{(X)}$ for each stock X over the historical time period 01/04/2016 though 01/02/2024 is a semi-martingale – most probably a Lévy process. Using the historical price series, we computed the time series of ESG-adjusted prices $A_t(\gamma)$ (8) over the range of parameter values $\gamma \in [-5,5]$. For each value of γ, we determined the signal:noise ratio, s:n(γ), of $A_t(\gamma)$. Fig. 4 shows plots of s:n(γ) for four example stocks, illustrating a range of behaviors.

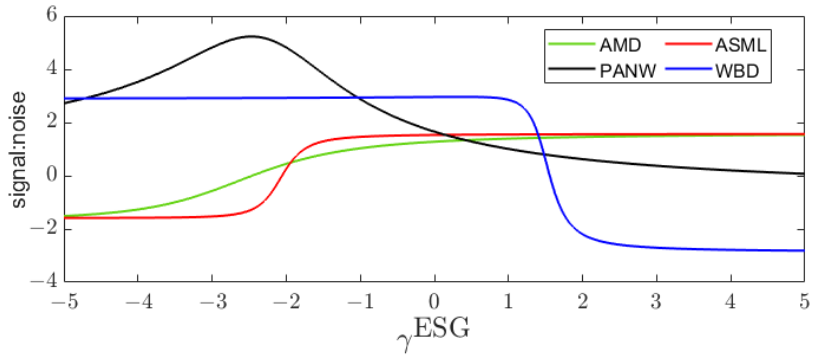

Figure 4 Signal:noise ratio as a function of γ.

Defining γ_l and γ_u by

$$\begin{aligned} \gamma_l &= \max\left\{\gamma < 0 \;:\; \left|\frac{\text{s:n}(\gamma)}{\text{s:n}(0)} - 1\right| = 0.05,\right\}, \\ \gamma_u &= \min\left\{\gamma > 0 \;:\; \left|\frac{\text{s:n}(\gamma)}{\text{s:n}(0)} - 1\right| = 0.05,\right\}, \end{aligned} \tag{31}$$

determines a range $\gamma \in [\gamma_l, \gamma_u]$ of values for which s:n(γ) lies withing 5% of the value s:n(0). We assumed that as long as the s:n ratio of the ESG-adjusted price $A_t(\gamma)$ remains within this range, the time series $A_t(\gamma)$ will continue to be a semi-martingale.[16]

The range $[\gamma_l, \gamma_u]$ found for each stock is given in Table A1 in Appendix H. The ranges vary, sometimes significantly. For the four stocks represented in Fig. 4, Fig. 5 plots the ESG-adjusted price series for $\gamma \in \{\gamma_l, 0, \gamma_h\}$. For PANW, the s:n ratio changes rapidly near $\gamma = 0$, and the range $[\gamma_l, \gamma_u]$ is very narrow. WBD and ASML illustrate that the s:n ratio can remain within 5% of s:n(0) for extended ranges of either $\gamma < 0$ or $\gamma > 0$. The results for AMD are representative of 13 of the 16 stocks for which $[\gamma_l, \gamma_u] \subset [-1,1]$. For AMD and ASML, $Z_t^{(X)} > Z_t^{()}$ (Fig. 2) over the historical time period; as a consequence the ESG-adjusted price increases with γ. For WBD, $Z_t^{(\text{WBD})} < Z_t^{()}$ and its ESG-adjusted stock price decreases as γ increases. PANW is the only stock of the 16 companies considered whose

[16] This does not imply an assumption that $A_t(\gamma)$ is not a semi-martingale if γ falls outside of the range $[\gamma_l, \gamma_u]$.

Preprints.org (www.preprints.org) | NOT PEER-REVIEWED | Posted: 6 February 2025 doi:10.20944/preprints202502.0372.v1

ESG score $Z_t^{(\mathrm{PANW})}$ increased from below to above that of . The $\gamma_l = -0.09$ and $\gamma_u = 0.09$ curves therefore cross each other near the start of 2022 (difficult to visualize in the plot for PANW in Fig. 5).

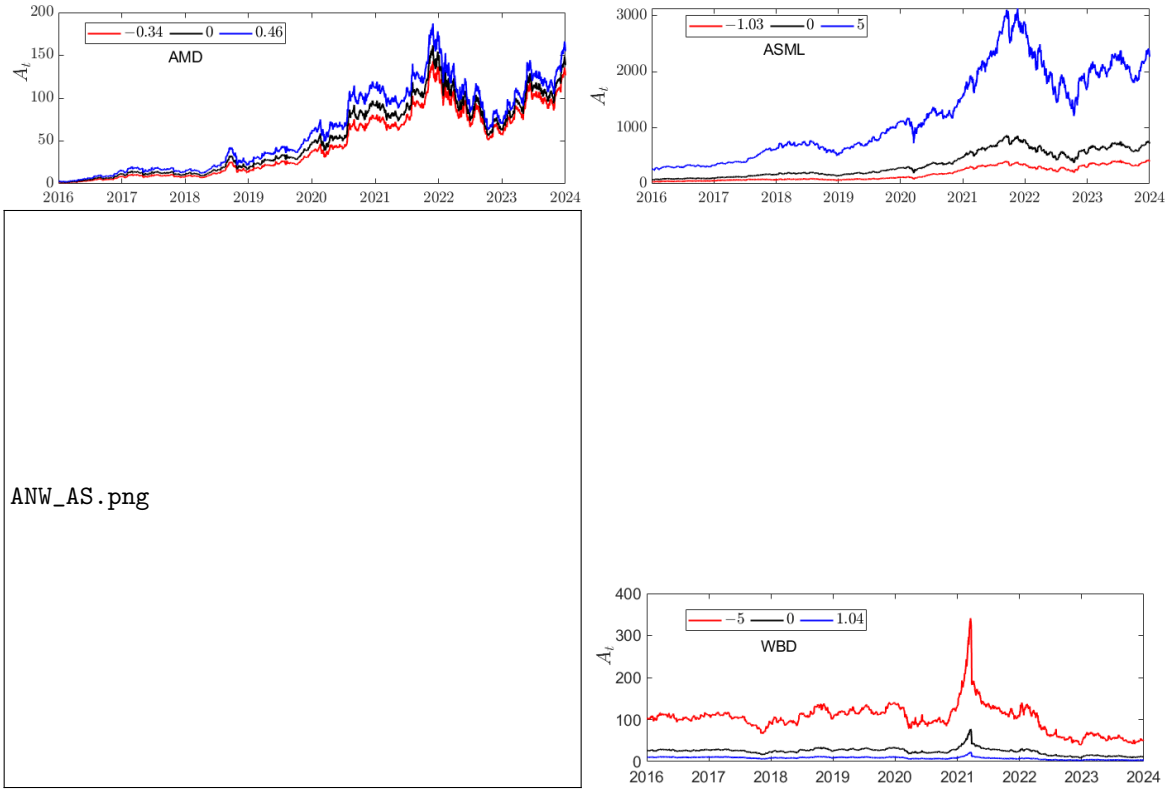

Figure 5 ESG-adjusted prices of the indicated stocks as γ is varied over the set of values $\{\gamma_l, 0, \gamma_h\}$.

4.3. Parameter fits

To compute option prices using the binomial BBSM model in Section 3, predictive empirical ESG-adjusted prices (10) were computed assuming constant parameter values. Lindquist et al. (2024, Section 9) suggested (but did not implement) procedures for fitting the parameters of a BBSM model. With minor modification, we follow their suggested procedure for estimating the risky-asset price parameters; we utilize a different procedure for estimating the riskless asset price parameters. The parameter values were estimated from the historical price data, as follows. Express the historical data as the trading dates $j = -M+1, \ldots, -1, 0$ ($M = 2{,}013$), where $j = -M+1$ corresponds to 01/04/2016 and $j = 0$ to 01/02/2024.[17] From (15) with constant coefficients, the conditional mean and variance of the discrete change in stock price are

$$\begin{aligned} \mathbb{E}\left[c_{(k+1)\Delta,n} | \mathcal{F}_k^{(n)}\right] &= (a + \mu A_{k\Delta,n})\,\Delta, \\ \mathrm{Var}\left[c_{(k+1)\Delta,n} | \mathcal{F}_k^{(n)}\right] &= (v + \sigma A_{k\Delta,n})^2\,\Delta. \end{aligned} \tag{32}$$

The parameters a and μ were obtained using the regression

$$\frac{c_{(j+1)\Delta,n}}{\Delta} = a + \mu A_{j\Delta,n} + \epsilon_{j\Delta,n}^{(1)}, \quad j = -M+1, \ldots, -1. \tag{33}$$

[17] The date 01/02/2024 (i.e. $j = 0$) corresponds to the date for which option price data was collected and used in Section 5 to compute implied ESG affinity values.

 doi:10.20944/preprints202502.0372.v1

Using the approximation $(c_{(k+1)\Delta,n})^2 \approx \mathrm{Var}\left[c_{(k+1)\Delta,n}|\mathcal{F}_k^{(n)}\right]$, the parameters v and σ were estimated from the regression

$$\frac{|c_{(j+1)\Delta,n}|}{\sqrt{\Delta}} = v + \sigma A_{j\Delta,n} + \epsilon^{(2)}_{j\Delta,n}, \qquad j = -M+1, \ldots, -1. \tag{34}$$

With constant parameters, the price dynamics (12) of the riskless asset has the discrete form[18]

$$\beta_{k\Delta,n} = \beta_{(k-1)\Delta,n} + \rho\Delta + r\Delta\beta_{(k-1)\Delta,n}. \tag{35}$$

The parameters ρ and r were estimated from the regression

$$\frac{\beta_{(j+1)\Delta,n} - \beta_{j\Delta,n}}{\Delta} = \rho + r\beta_{j\Delta,n} + \delta_{j\Delta,n}, \qquad j = -M+1, \ldots, -1. \tag{36}$$

The sequence of daily values $\beta_{j\Delta,n}$ required in (36) was generated as follows:

$$\beta_{(j+1)\Delta,n} = (1 + r_{3,j}\Delta)\beta_{j\Delta,n}, \quad j = -M+1, \ldots, -1, \ \beta_{(-M+1)\Delta,n} = A_{(-M+1)\Delta,n}, \tag{37}$$

where $r_{3,j}$ is the three-month U.S. Treasury bill rate, converted to a daily rate.[19,20]

Finally, we estimated the probability p_n for the upward movement of the daily ESG-adjusted closing price by

$$p_n = \frac{1}{M-1} \sum_{j=-M+2}^{0} I_{c_{j\Delta,n}>0}, \tag{38}$$

where the indicator function $I_{x>0}$ satisfies $I_{x>0} = 1$ if $x > 0$ and $I_{x>0} = 0$ otherwise.

From (8), for each time t there exists a value $\gamma_{0,t}^{\mathrm{ESG}} = -1/Z_t^{(X;I)} \in \mathbb{R}$ such that $A_t = S_t^{(X)}\left(1 + \gamma_{0,t} Z_t^{(X;I)}\right) = 0$. Therefore if $Z_t^{(X;I)} = Z^{(X;I)}$, a time independent constant over the historical period for which the regression fits (33) and (34) are to be attempted, the linear regressions near the value $\gamma_0^{\mathrm{ESG}} = -1/Z^{(X;I)}$ become ill-conditioned and unrealistic parameter fits result. As we utilized an eight-year historical window over which $Z_t^{(X;I)}$ had behaviors similar to that illustrated in Fig. 3, this was not an issue.

Fig. 6 shows the dependence of the values of the fitted parameters $\hat{a}, \hat{\mu}, \hat{v}, \hat{\sigma}, \hat{\rho}, \hat{r}, \hat{p}_n$ on $\gamma \in [\gamma_l, \gamma_u]$ for ASML and ROST. These are illustrative of the forms of dependence seen in the 16 stocks. In the plots for $\hat{p}_n$, the black curve indicates the value of p_n estimated using (38). A change in the value of $I_{c_{j\Delta,n}>0}$ by its smallest increment (± 1) as γ changes is visible as a corresponding jump in the value of $\hat{p}_n$. We used a Gaussian-weighted, moving average smoother (with a window of 21 days) to smooth the $\hat{p}_n$ values (red curve).

In (37) the value of γ only affects the value of $A_{(-M+1)\Delta,n}$. Consequently, in the fit (36) we see from Fig. 6 that the parameter ρ depends on γ, while the parameter r is independent of the value γ. In fact the constant fitted value of $\hat{r}$ is independent of the stock considered, which makes sense as, except for an initial value $\beta_{(-M+1)\Delta,n} = A_{(-M+1)\Delta,n}$, (37) and (36) depend only on the riskless asset.

Fig. 6 shows that, with the exception of $\hat{r}$, as γ varies over the range $[\gamma_l, \gamma_u]$, each fitted parameter varies over a range of values, with the range varying by stock. For each fitted parameter, Fig. 7 compares, by stock, the range of values taken on by that parameter. Dotted horizontal lines are used to guide the eye to separate positive from negative paramater ranges, or, in the case of $\hat{p}_n$, to indicate

[18] We note that the recursion relation (35) has the solution $\beta_{k\Delta,n} = (1+r\Delta)^k\beta_0 + \rho\Delta\sum_{j=0}^{k-1}(1+r\Delta)^j$. Under the limits $k \uparrow \infty$, $\Delta \downarrow 0$, such that $k\Delta = \tau$, where τ is a constant time, the limit of this discrete solution is $\beta_\tau = e^{r\tau}\beta_0 + \rho/r[e^{r\tau} - 1]$, in agreement with the continuous solution to (2) under constant coefficients.

[19] In effect, equation (36) models the evolution of the yield of the three-monthy Treasury bill using the discrete form (35) of the BBSM model riskless rate dynamics (2).

[20] Source: https://home.treasury.gov/resource-center/data-chart-center/interest-rates/TextView?type=daily_treasury_yield_curve&field_tdr_date_value=2024. Accessed 01/02/2024.

Preprints.org (www.preprints.org) | NOT PEER-REVIEWED | Posted: 6 February 2025 doi:10.20944/preprints202502.0372.v1

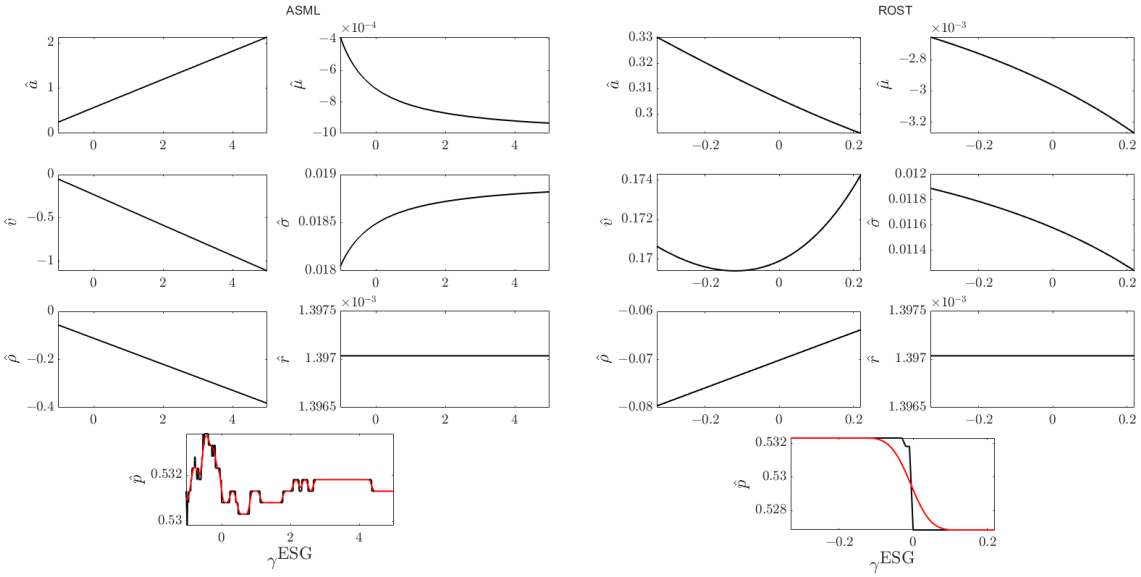

Figure 6 AMD and ROST parameter dependence on γ over their respective ranges $[\gamma_l, \gamma_u]$.

stocks having $p_n > 0.5$. We note that the range $[\gamma_l, \gamma_u]$ for each stock includes $\gamma = 0$ (no ESG price adjustment). Even so, the MB parameters $\hat{a}$, $\hat{v}$ and $\hat{\rho}$ are consistently different from 0 over the full $[\gamma_l, \gamma_u]$ range (except for $\hat{v}$ for WBD). Thus the parameter fits, even for the financial stock price ($\gamma = 0$), show an admixture of MB and BSM behavior. The values of $\hat{a}$ and $\hat{\sigma}$ are positive for all 16 stocks; for $\hat{\rho}$ all values are negative. For $\hat{\mu}$, all are negative except for two stocks, NVDA and PANW. Values of $\hat{v}$ are equally divided between positive and negative over the 16 stocks. Values of $\hat{p}_n$ exceed 0.5 for all stocks except WBD.

5. The Implied ESG Affinity

Let $C^{(\mathrm{emp})}(A_0, T_i, K_j)$ denote published call option prices for an underlying stock having maturity date T_i, $i \in I$, and strike price K_j, $j \in J$. Let $C^{(\mathrm{th})}\left(A_0, T_i, K_j; a, \mu, v, \sigma, \rho, r, p_n, \gamma\right)$ denote the call option price computed from Section 3 with constant parameters values. Let $\hat{\xi}$ denote the historical estimation of any parameter ξ. (Recall that, except for $\hat{r}$, the parameters have dependence on the value of γ.) Then implied values for γ are computed via

$$\gamma^{(,\mathrm{imp})}(T_i, K_j) =_{\gamma} \left(\frac{C^{(\mathrm{th})}\left(A_0, T_i, K_j; \hat{a}, \hat{\mu}, \hat{v}, \hat{\sigma}, \hat{\rho}, \hat{r}, \hat{p}_n, \gamma\right) - C^{(\mathrm{emp})}(A_0, T_i, K_j)}{C^{(\mathrm{emp})}(A_0, T_i, K_j)} \right)^2, \tag{39}$$

Based upon call option prices published on 01/02/2024,[21] we computed theoretical call option prices for the same set of strike prices, K_j, $j \in J$, and maturity times T_i, $i \in I$. In (39), the parameters $\hat{a}, \hat{\mu}, \hat{v}, \hat{\sigma}, \hat{\rho}, \hat{p}_n$ used in the theoretical option computation were fit from the historical data for each value of γ tested in the minimization procedure. As the value of $\hat{r}$ is independent of the value of γ and of the stock, theoretically it only needed to be calculated once. However, it is computed from the same regression (36) that produces $\hat{\rho}$, so it was recomputed for each value of γ tested. The value $Z_t^{(\mathrm{X},)}$ used to compute prices on the binomial tree was the smoothed value for 01/02/2024.

[21] Source: Yahoo Finance. Accessed 01/02/2024.

Preprints.org (www.preprints.org) | NOT PEER-REVIEWED | Posted: 6 February 2025 doi:10.20944/preprints202502.0372.v1

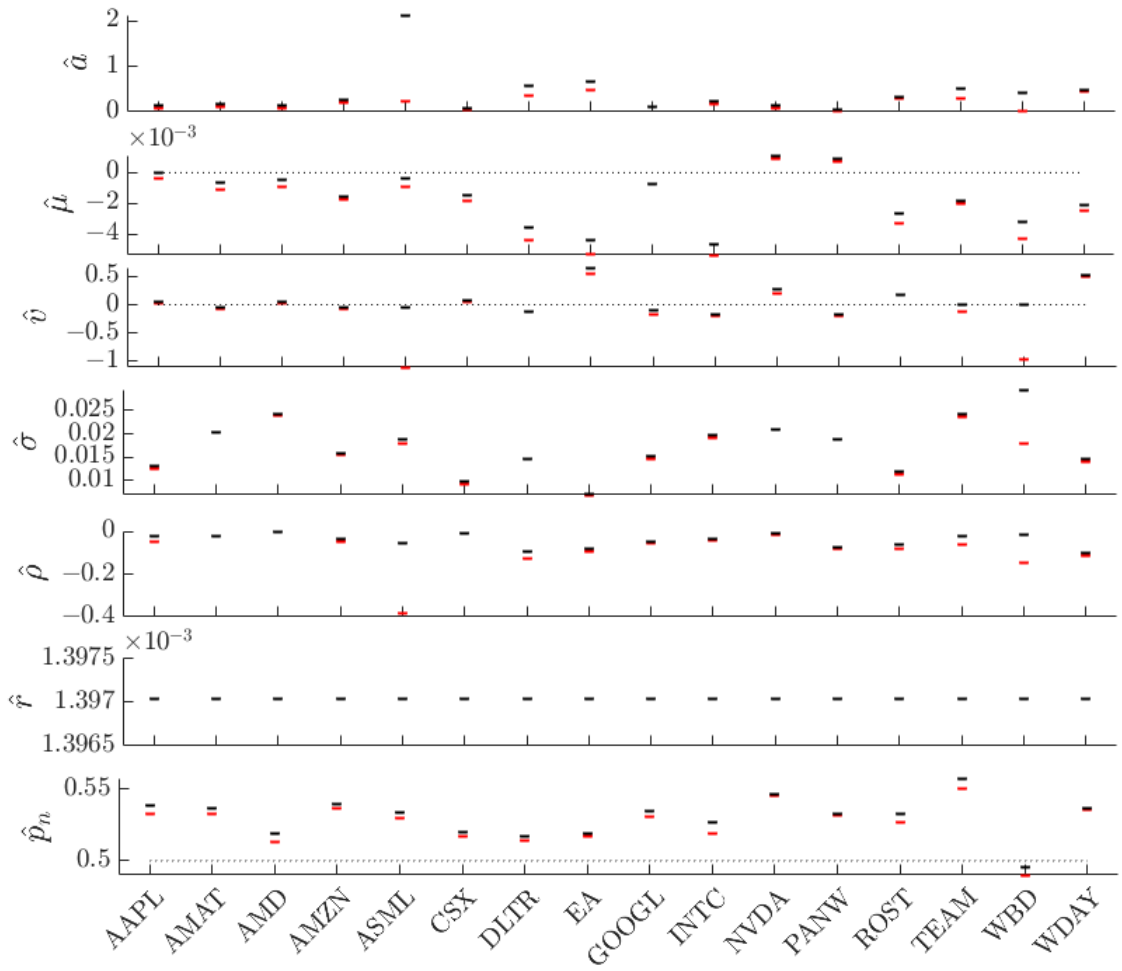

Figure 7 Range of fitted parameter values, by stock. The upper value of each range is black, the lower value is red. Dotted horizontal lines denote the value 0 or 0.5 as appropriate.

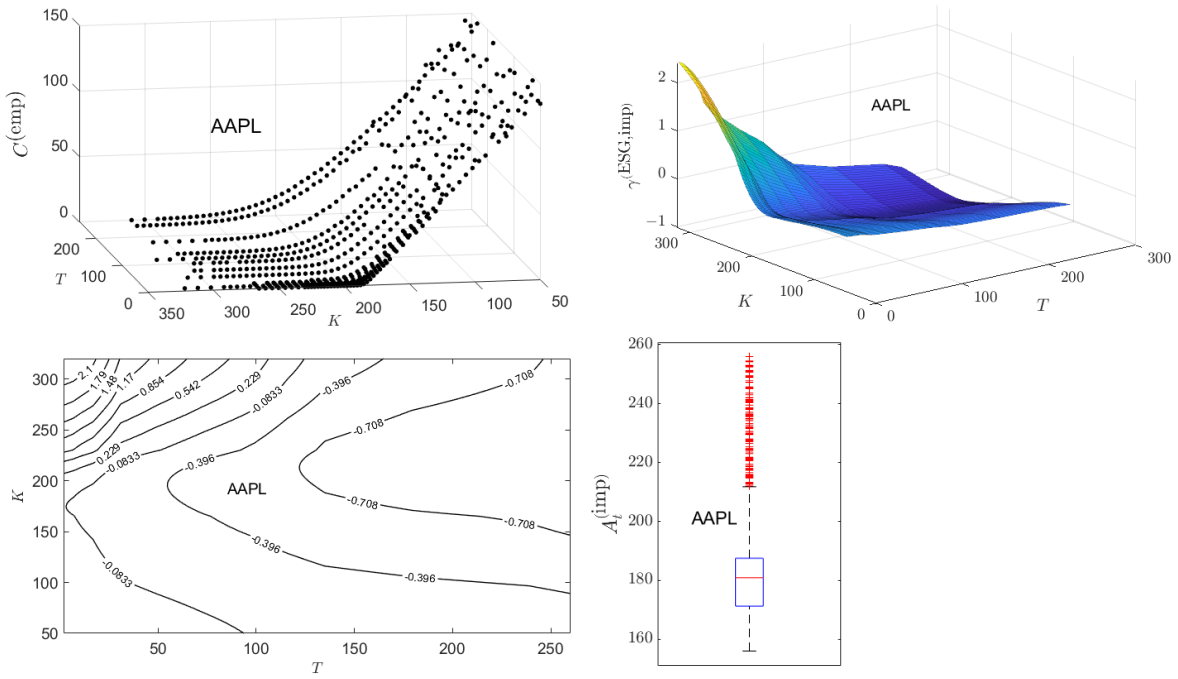

Figure 8 For the stock AAPL: (top left) The empirical option prices published for AAPL on 01/02/2024. (top right) The computed surface of $\gamma^{(,\mathrm{imp})}$ values. (bottom left) Contours of the $\gamma^{(,\mathrm{imp})}$ surface. (bottom right) Box-whisker summary of the distribution of $\gamma^{(,\mathrm{imp})}$ values.

Preprints.org (www.preprints.org) | NOT PEER-REVIEWED | Posted: 6 February 2025 doi:10.20944/preprints202502.0372.v1

The published call option prices for AAPL on 01/02/2024 are presented in Fig. 8.[22] In contrast to some of the other stocks investigated, these option prices form a fairly "regular" surface over the published range of K_j, $j \in J^{(\text{AAPL})}$, and maturity times T_i, $i \in I^{(\text{AAPL})}$ values. The values $\gamma^{(,\text{imp})}(T_i, K_j)$ computed from (39) are plotted as a surface in Fig. 8.[23] Analysis of the $\gamma^{(,\text{imp})}$ surface is enhanced by consideration of surface contours as shown in the bottom left of the figure. The $\gamma^{(,\text{imp})}(T, K) = 0$ contour lies between the contours -0.0833 and 0.229, indicating that option traders have a positive view (relative to) of the ESG rating of AAPL in the upper left triangular region of out-of-the money (the adjusted closing price for AAPL on 01/02/2024 was \$185.64) strike prices and maturity dates not exceeding 110 trading days. However, over the majority of (T, K) values, the option traders have a negative view of the ESG rating of AAPL.

A further view of the $\gamma^{(,\text{imp})}$ values is presented in Fig. 8 as a box-whisker summary of the distribution over the surface. Table A1 in Appendix H presents the numerical values of the minumum, maximum, P_{25}, P_{50}, and P_{75} percentiles of the $\gamma^{(,\text{imp})}$ distribution for AAPL. This table also presents the $[\gamma_l, \gamma_u]$ for AAPL based upon examination of historical adjusted ESG prices discussed in Section 4.3. The overwhelming majority of $\gamma^{(,\text{imp})}$ values lie within the $[\gamma_l, \gamma_u]$ for AAPL, giving some confidence that the implied ESG affinity values being computed are consistent with semi-martingale behavior of the associated ESG-adjusted price.

To appreciate the implication of this, we define from (8) an implied ESG-adjusted price

$$A_t^{(\text{imp})} = S_t^{(X)}\left(1 + \gamma^{(\text{ESG;imp})} Z_t^{(X;)}\right), \tag{40}$$

where, for a given stock X, $\gamma^{(\text{ESG;imp})}$ is a value from the implied ESG affinity surface, and $Z_t^{(X;)}$ was the relative ESG score and $S_t^{(X)}$ the spot price price used in computing the surface.

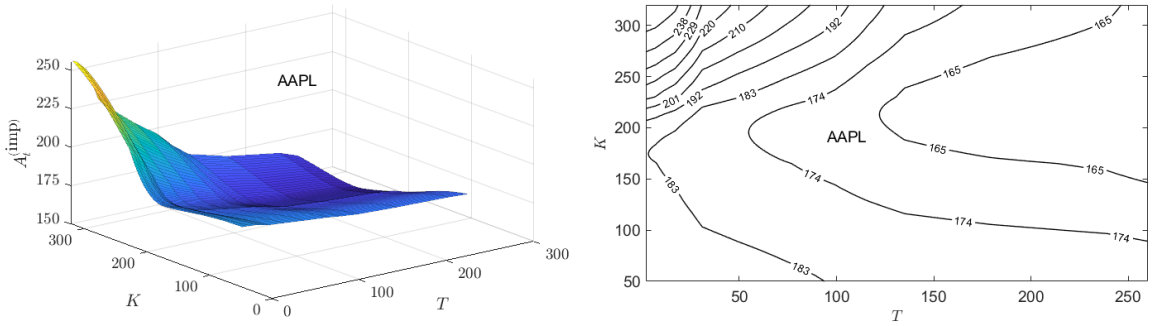

Figure 9 For the stock AAPL: (left) The computed surface of $A_t^{(\text{imp})}$ values. (right) Contours of the $A_t^{(\text{imp})}$ surface.

Fig. 9 presents the surface of $A_t^{(\text{imp})}$ values computed from the $\gamma^{(,\text{imp})}$ values of Fig. 8. Also shown are contour levels of the $A_t^{(\text{imp})}$ corresponding to the analogous contour levels of $\gamma^{(,\text{imp})}$ shown in Fig. 8. Whether $A_t^{(\text{imp})}$ is larger or smaller than $S_t^{(X)}$ depends on the sign of the product $\gamma^{(\text{ESG;imp})} Z_t^{(X;)}$. If $Z_t^{(X;)}$ is positive, then positive values of $\gamma^{(\text{ESG;imp})}$ correspond to an ESG valuation that exceeds $S_t^{(X)}$. However, if $Z_t^{(X;)}$ is negative, then negative values of $\gamma^{(\text{ESG;imp})}$ correspond to an ESG valuation that exceeds $S_t^{(X)}$. Thus, consideration of the $A_t^{(\text{imp})}$ surfaces rather than the $\gamma^{(\text{ESG;imp})}$ surfaces provides direct insight into the views of option traders on the ESG-valuation of stocks.

Since $Z_t^{(\text{AAPL},)}$ was positive on 01/02/2024, the surfaces of $\gamma^{(,\text{imp})}$ and $A_t^{(\text{imp})}$ are identical except for a rescaling of the z-axis. Similarly the contour plots for $\gamma^{(,\text{imp})}$ and $A_t^{(\text{imp})}$ are identical except for a

[22] In all plots, the maturity times T are presented in terms of trading days post 01/02/2024.

[23] In preparing the final surface shown, triangulation-based nearest neighbor interpolation was used to fill in missing (T_i, K_j) values in the $\gamma^{(,\text{imp})}$ surface. The surface was then smoothed using a Gaussian weighted, moving average algorithm. This smoothing produced relatively minor changes.

 doi:10.20944/preprints202502.0372.v1

rescaling of the value on the contour levels. The negative view of the option traders over most of the (T, K) range for AAPL, results in implied, ESG-adjusted prices for 01/02/2024 that correspondingly fall below the financial price of AAPL on 01/02/2024.

Figs. B1 and B2 in Appendix I plot the published option prices on 01/02/2024 for all 16 stocks studied. The eight stocks for which $Z_t^{(X;)} > 0$ on $t = 01/02/2024$ are presented in Fig. B1, while the eight stocks for which $Z_t^{(X;)} < 0$ are presented in Fig. B2. This separation reflects the fact that when $Z_t^{(X;)} > 0$, the corresponding surfaces for $\gamma^{(,\text{imp})}$ and $A_t^{(\text{imp})}$ will look like identical (rescaled) versions of each other. However, when $Z_t^{(X;)} < 0$, the surface $A_t^{(\text{imp})}$ will look like an inverted, rescaled version of the corresponding $\gamma^{(,\text{imp})}$ surface. Examination of published option prices for PANW, TEAM, and WDAY show much greater irregularity over the range of K and T values than that shown for AAPL.[24]

Plots of the $\gamma^{(,\text{imp})}$ surfaces for all 16 stocks are presented in Figs. C1 and C2 in Section J. The stock organization into two panels mirrors that for Figs. B1 and B2. Figs. C3 and C4 provide the contour plots of these surfaces. Plots of the $A_t^{(\text{imp})}$ surfaces for all 16 stocks are presented in Figs. D1 and D2 in Section K. Figs. D3 and D4 provide the contour plots of these surfaces.

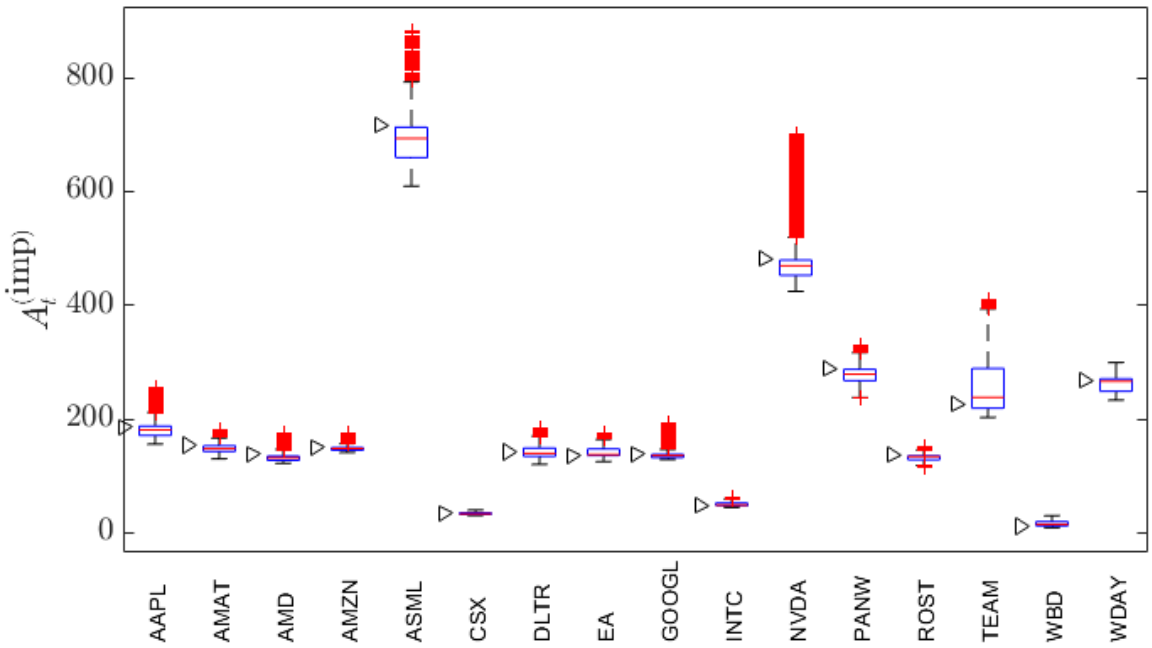

Figure 10 Box-whisker summaries of the distribution of $A_t^{(\text{imp})}$ values for all 16 stocks studied. The "right-arrow" to the left of each box-whisker plot for $A_t^{(\text{imp})}$ corresponds to the stock spot price on 01/02/2024.

To summarize the information in Appendices J and K, Fig. 10 presents the box-whisker summaries of the distributions of $A_t^{(\text{imp})}$ values for each of the 16 stocks. (The corresponding box-whisker summaries of the distributions of $\gamma^{(,\text{imp})}$ values are given in Fig. C5.) Also indicated just to the left of each box-whisker summary is the financial spot price of the stock on 01/02/2024. For ease of reference, the financial spot prices on 01/02/2024 are listed in Table A2. From the contour plots in Figs. D3 and D4, one can then ascertain over what region of (T, K) values option traders view the ESG valuation of the stock to be higher than its financial price. For EA, INTC, TEAM and WBD, spot traders have an implied ESG valuation that exceeds the spot price over most of the (T, K) region. For eight of the stocks (AAPL, AMAT, AMD, AMZN, ASML, CSX, NVDA, PANW), the implied ESG valuation exceeds the spot price over a triangular, out-of-the-money, shorter maturity time region as described above for AAPL. For the remaining four stocks, the implied ESG valuation exceeds the spot price over most

[24] This results in some corresponding surface irregularity (even after smoothing) in the $\gamma^{(,\text{imp})}$ surface.

 doi:10.20944/preprints202502.0372.v1

of the out-of-the-money region. Thus, for 12 of the 16 stocks, option traders have in-the-money ESG valuations that are lower than the spot price.

6. Trading Forward Contracts Utilizing Information on Asset Price Direction

Hu et al. (2020) extended BSM-based binomial option pricing theory to complete markets containing traders that have information on the stock price direction. We further extend that theory using the BBSM-based binomial option pricing in complete markets of Section 3. For simplicity, we assume the parameters in the BBSM binomial model are constant: $a_{k\Delta,n} = a$, $\mu_{k\Delta,n} = \mu$, $v_{k\Delta,n} = v$, $\sigma_{k\Delta,n} = \sigma$, $\rho_{k\Delta,n} = \rho$, and $r_{k\Delta,n} = r$, $Z^{(X,I)}_{k\Delta,n} = Z^{(X,I)}$. As earlier, we continue to assume γ is constant.

Let $\aleph$ denote the trader (hedger) holding the short position in the option contract. Let $p^{\aleph}_n \in (0,1)$ denote the probability that information held by $\aleph$ at time $k\Delta$, $k = 0, ..., n-1$, on the direction of stock price movement within any interval $[k\Delta, (k+1)\Delta]$ is correct. If $p^{\aleph}_n > 1/2$, $\aleph$ is an informed trader; if $p^{\aleph}_n < 1/2$, $\aleph$ is misinformed; and if $p^{\aleph}_n = 1/2$, we refer to $\aleph$ as a noisy trader. We assume $\aleph$ is the only informed trader in a market of noisy traders; consequently, $\aleph$'s informed trading actions do not influence market prices.

In Hu et al. (2020), Shannon's entropy (see e.g., Rioul 2018; Robinson 2008) is used to quantify the amount of information $\aleph$ possesses. As with the price movement probability p_n of Section 3, $p^{\aleph}_n$ is the probability governing a Bernoulli random variable $\eta_{k,n}$ such that $\mathbb{P}(\eta_{k,n} = 1) = 1 - \mathbb{P}(\eta_{k,n} = 0) = p^{\aleph}_n$. Then Shannon's entropy is $H(p^{\aleph}_n) = -p^{\aleph}_n \ln p^{\aleph}_n - (1-p^{\aleph}_n)\ln(1-p^{\aleph}_n)$, having maximum value $H(1/2) = \ln 2$. Hu et al. (2020) defined $\aleph$'s level of information as[25]

$$\tau(p^{\aleph}_n) = \text{sign}(p^{\aleph}_n - 1/2)\frac{H(1/2) - H(p^{\aleph}_n)}{H(p^{\aleph}_n)}, \tag{41}$$

where

$$\text{sign}(p^{\aleph}_n - 1/2) = \begin{cases} 1, & \text{if } 1/2 < p^{\aleph}_n \le 1, \\ 0, & \text{if } p^{\aleph}_n = 1/2, \\ -1, & \text{if } 0 \le p^{\aleph}_n < 1/2. \end{cases} \tag{42}$$

We address the question of $\aleph$'s potential gain from trading with an information level $\tau(p^{\aleph}_n) > 0$. At any time $k\Delta$, $k = 0, \ldots, n-1$, $\aleph$ makes independent bets, $\eta_{k+1,n}$, $k = 0, \ldots, n-1$. Thus, the filtration (11) needs to be augmented with the sequence of $\aleph$'s independent bets:

$$\mathbb{F}^{(n;\aleph)} = \{\mathcal{F}^{(n,\aleph)}_k = \sigma(\zeta_{j,n}, \eta_{j,n} : j = 1, ..., k),\ \mathcal{F}^{(n,\aleph)}_0 = \{\emptyset, \Omega\}\}. \tag{43}$$

Specifically, relying on the information on stock-price direction, $\aleph$ adopts a trading strategy involving forward contracts. For convenience, we label the two scenarios given by (10) for the price of $\mathcal{A}$:

$S^{(\text{up})}_c$: $\zeta_{k+1,n} = 1$, resulting in $A_{(k+1)\Delta,n} = A_{k,n} + u_{k\Delta,n}$ w.p. p_n,

$S^{(\text{down})}_c$: $\zeta_{k+1,n} = 0$, resulting in $A_{(k+1)\Delta,n} = A_{k,n} + d_{k\Delta,n}$ w.p. $1 - p_n$,

where $u_{k\Delta,n}$ and $d_{k\Delta,n}$ are given by (16) with constant coefficients. If at $k\Delta t$, $\aleph$ believes that $S^{(\text{up})}_c$ will happen, $\aleph$ takes a long position[26] in $\Delta^{(\aleph)}_{k\Delta}$-forward contracts, for some $\Delta^{(\aleph)}_{k\Delta} >\in \mathbb{R}_+$.[27] The forward contracts mature at $(k+1)\Delta$. If at $k\Delta$, $\aleph$ believes that $S^{(\text{down})}_c$ will happen, then $\aleph$ takes a short position in $\Delta^{(\aleph)}_{k\Delta t}$-forward contracts[26] having maturity $(k+1)\Delta$.

---

[25] Hu et al. (2020) write (41) in terms of the information distance

$$D(p^{\aleph}_n, 1/2) = H(1/2) - H(p^{\aleph}_n) = p^{\aleph}_n \ln(2p^{\aleph}_n) + (1-p^{\aleph}_n)\ln(2(1-p^{\aleph}_n)).$$

[26] The opposite party to this transaction is a noisy trader.

[27] An optimal value for $\Delta^{(\aleph)}_{k\Delta}$ is determined below.

 doi:10.20944/preprints202502.0372.v1

Lindquist et al. (2024) developed the price of a forward contract under the BBSM model. Assuming there is no initial cost to enter into the forward contract and constant coefficients, the T-forward price of $\mathcal{A}$ is

$$F(t,T) = A_t \exp\left\{\int_t^T \left(r + \frac{\rho}{\beta_s}\right) ds\right\}, \tag{44}$$

where the constant coefficient solution to (2) is (Lindquist et al. 2024, (A3))

$$\beta_t = \begin{cases} (\beta_0 + \rho/r)e^{rt} - \rho/r \text{ if } r \neq 0, \\ \beta_0 + \rho t \qquad\qquad\quad \text{if } r = 0. \end{cases} \tag{45}$$

Evaluating (44) using (45) gives

$$F(t,T) = A_t \frac{\beta_T}{\beta_t}, \tag{46}$$

for all $r \in \mathbb{R}$. Discretizing (46) over the time interval $k\Delta \to (k+1)\Delta$ and assuming $o(\Delta) = 0$, (46) becomes

$$\begin{aligned} F(k\Delta,(k+1)\Delta) &= A_{k\Delta}\frac{\beta_{(k+1)\Delta}}{\beta_{k\Delta}} \\ &= A_{k\Delta}\frac{(\beta_{k\Delta}+\rho/r)e^{r\Delta} - \rho/r}{\beta_{k\Delta}} \\ &= A_{k\Delta}(1 + [r + \rho/\beta_{k\Delta}]\Delta). \end{aligned} \tag{47}$$

For notational brevity, define $\searrow_{k\Delta} = r + \rho/\beta_{k\Delta}$.

Using (10), conditionally on $\mathcal{F}_k^{(n,\aleph)}$, the payoff possibilities of $\aleph$'s forward contract positions can be written

$$\begin{aligned} P^{(\aleph;\text{forward})}_{k\Delta\to(k+1)\Delta} \mid \mathcal{F}_k^{(n,\aleph)} &= \Delta_{k\Delta}^{(\aleph)} \begin{cases} A^{(u)}_{(k+1)\Delta,n} - A_{k\Delta,n}(1+\searrow_{k\Delta}\Delta) & \text{w.p. } p_n p_n^{(\aleph)}, \\ A_{k\Delta,n}(1+\searrow_{k\Delta}\Delta) - A^{(d)}_{(k+1)\Delta,n} & \text{w.p. } (1-p_n)p_n^{(\aleph)}, \\ A_{k\Delta,n}(1+\searrow_{k\Delta}\Delta) - A^{(u)}_{(k+1)\Delta,n} & \text{w.p. } p_n\left(1-p_n^{(\aleph)}\right), \\ A^{(d)}_{(k+1)\Delta,n} - A_{k\Delta,n}(1+\searrow_{k\Delta}\Delta) & \text{w.p. } (1-p_n)\left(1-p_n^{(\aleph)}\right), \end{cases} \\ &= \Delta_{k\Delta}^{(\aleph)} \begin{cases} u_{k\Delta,n} - A_{k\Delta,n}\searrow_{k\Delta}\Delta & \text{w.p. } p_n p_n^{(\aleph)}, \\ A_{k\Delta,n}\searrow_{k\Delta}\Delta - d_{k\Delta,n} & \text{w.p. } (1-p_n)p_n^{(\aleph)}, \\ A_{k\Delta,n}\searrow_{k\Delta}\Delta - u_{k\Delta,n} & \text{w.p. } p_n\left(1-p_n^{(\aleph)}\right), \\ d_{k\Delta,n} - A_{k\Delta,n}\searrow_{k\Delta}\Delta & \text{w.p. } (1-p_n)\left(1-p_n^{(\aleph)}\right). \end{cases} \end{aligned} \tag{48}$$

The conditional expected payoff is

$$\begin{aligned} &E\left[P^{(\aleph;\text{forward})}_{k\Delta\to(k+1)\Delta} \mid \mathcal{F}_k^{(n,\aleph)}\right] \\ &\qquad = \Delta_{k\Delta}^{(\aleph)}\left(2p_n^{\aleph} - 1\right)[p_n u_{k\Delta,n} - (1-p_n)d_{k\Delta,n} + (1-2p_n)A_{k,n}\searrow_{k\Delta}\Delta], \end{aligned} \tag{49}$$

with $u_{k\Delta,n}$ and $d_{k\Delta,n}$ given by (16).

We write

$$p_n^{\aleph} = \frac{(1 + \lambda_\Delta^{(\aleph)}\sqrt{\Delta})}{2}, \tag{50}$$

 doi:10.20944/preprints202502.0372.v1

where, $0 < \lambda_{\Delta}^{(\aleph)}\sqrt{\Delta} \leq 1$, for any finite value of Δ. $\lambda_{\Delta}^{(\aleph)}$ is referred to as $\aleph$'s information intensity. Again assuming $o(\Delta) = 0$,[28]

$$E\left[P_{k\Delta\to(k+1)\Delta}^{(\aleph;\text{forward})} \mid \mathcal{F}_k^{(n,\aleph)}\right] = 2\sqrt{p_n(1-p_n)}\,\lambda_{\Delta}^{(\aleph)}\Delta_{k\Delta}^{(\aleph)}\psi_{k\Delta,n}\Delta. \tag{51}$$

Under the same assumption, the conditional variance of $\aleph$'s payoff is

$$\text{Var}\left[P_{k\Delta\to(k+1)\Delta}^{(\aleph;\text{forward})} \mid \mathcal{F}_k^{(n,\aleph)}\right] = \left(\Delta_{k\Delta}^{(\aleph)}\psi_{k\Delta,n}\right)^2\Delta. \tag{52}$$

The instantaneous information ratio is then

$$IR\left(P_{k\Delta\to(k+1)\Delta}^{(\aleph;\text{forward})} \mid \mathcal{F}_k^{(n,\aleph)}\right) = \frac{E\left[P_{k\Delta\to(k+1)\Delta}^{(\aleph;\text{forward})} \mid \mathcal{F}_k^{(n,\aleph)}\right]}{\sqrt{\text{Var}\left[P_{k\Delta\to(k+1)\Delta}^{(\aleph;\text{forward})} \mid \mathcal{F}_k^{(n,\aleph)}\right]\Delta}} = 2\sqrt{p_n(1-p_n)}\lambda_{\Delta}^{(\aleph)}. \tag{53}$$

As $\lambda_{\Delta}^{(\aleph)}$ is positive, the information ratio on the payoff of $\aleph$'s strategy increases: as $\aleph$'s information intensity increases, and when $p_n \to 1/2$.[29]

To hedge the short position in the option, $\aleph$ executes the positions (17), while simultaneously running the futures trading strategy. This leads to an enhanced price process for $\aleph$, the dynamics of which can be expressed as:

$$A_{(k+1)\Delta,n}^{(\aleph)} = \begin{cases} A_{(k+1)\Delta,n}^{(u)} + \Delta_{k\Delta}^{(\aleph)}\left(A_{(k+1)\Delta,n}^{(u)} - A_{k\Delta,n}(1+\searrow_{k\Delta}\Delta)\right) & \text{w.p. } p_n p_n^{(\aleph)}, \\ A_{(k+1)\Delta,n}^{(d)} + \Delta_{k\Delta}^{(\aleph)}\left(A_{k\Delta,n}(1+\searrow_{k\Delta}\Delta) - A_{(k+1)\Delta,n}^{(d)}\right) & \text{w.p. } (1-p_n)p_n^{(\aleph)}, \\ A_{(k+1)\Delta,n}^{(u)} + \Delta_{k\Delta}^{(\aleph)}\left(A_{k\Delta,n}(1+\searrow_{k\Delta}\Delta) - A_{(k+1)\Delta,n}^{(u)}\right) & \text{w.p. } p_n\left(1-p_n^{(\aleph)}\right), \\ A_{(k+1)\Delta,n}^{(d)} + \Delta_{k\Delta}^{(\aleph)}\left(A_{(k+1)\Delta,n}^{(d)} - A_{k\Delta,n}(1+\searrow_{k\Delta}\Delta)\right) & \text{w.p. } (1-p_n)\left(1-p_n^{(\aleph)}\right), \end{cases} \tag{54}$$

$k = 0, 1, \ldots, n-1$, $n\Delta = T$. The price change of the process (54) is

$$c_{(k+1)\Delta,n}^{(\aleph)} = A_{(k+1)\Delta,n}^{(\aleph)} - A_{k\Delta,n}, \qquad k = 0, \ldots, n-1, \quad c_{0,n}^{(\aleph)} = 0. \tag{55}$$

Conditionally on $\mathcal{F}_k^{(n,\aleph)}$, and using (16),

$$\begin{aligned} E\left[c_{k+1\Delta,n}^{(\aleph)}|\mathcal{F}_k^{(n,\aleph)}\right] &= \varphi_{k\Delta,n}\Delta + \Delta_{k\Delta}^{(\aleph)}\lambda_{\Delta}^{(\aleph)}\sqrt{p_n(1-p_n)}\,\psi_{k\Delta,n}\Delta\,, \\ \text{Var}\left[c_{k+1\Delta,n}^{(\aleph)}|\mathcal{F}_k^{(n,\aleph)}\right] &= \left(1+\left(\Delta_{k\Delta}^{(\aleph)}\right)^2\right)\psi_{k\Delta,n}^2\Delta\,. \end{aligned} \tag{56}$$

It is in $\aleph$'s interest to find the value of $\Delta_{k\Delta}^{(\aleph)}$ which maximizes the conditional Markowitz' expected utility function,

$$U\left(c_{(k+1)\Delta,n}^{(\aleph)}|\mathcal{F}_k^{(n,\aleph)}\right) = E\left[c_{(k+1)\Delta,n}^{(\aleph)}|\mathcal{F}_k^{(n,\aleph)}\right] - \alpha^{(\aleph)}\,\text{Var}\left[c_{(k+1)\Delta,n}^{(\aleph)}|\mathcal{F}_k^{(n,\aleph)}\right], \tag{57}$$

where $\alpha^{(\aleph)} \geq 0$ is $\aleph$'s risk-aversion parameter. Using (56), $U\left(c_{(k+1)\Delta,n}^{(\aleph)}|\mathcal{F}_k^{(n,\aleph)}\right)$ is maximized for

$$\Delta_{k\Delta t}^{(\aleph,\text{opt})} = \frac{\sqrt{p_n(1-p_n)}\,\lambda_{\Delta}^{(\aleph)}}{2\alpha^{(\aleph)}\psi_{k\Delta,n}}. \tag{58}$$

[28] It is sufficient to require terms of $o(\Delta)$ to vanish in order to apply invariance principles, such as that by Donsker and Prokhorov, to obtain the continuum limits of this discrete formulation.

[29] Expressed differently, when $p_n \downarrow 0$ or $p_n \uparrow 1$, the price movement becomes obvious to all traders and $\aleph$ can therefore be "no more informed" than a noisy trader.

 doi:10.20944/preprints202502.0372.v1

Under the optimal value,

$$\begin{aligned} E\left[c^{(\aleph)}_{(k+1)\Delta,n}|\mathcal{F}^{(n,\aleph)}_k\right] &= \varphi_{k\Delta,n}\Delta + \frac{p_n(1-p_n)}{2\alpha^{(\aleph)}}\left(\lambda^{(\aleph)}_\Delta\right)^2\Delta, \\ \mathrm{Var}\left[c^{(\aleph)}_{(k+1)\Delta,n}|\mathcal{F}^{(n,\aleph)}_k\right] &= [H(\aleph)\psi_{k\Delta,n}]^2\Delta, \\ H(\aleph) &= \sqrt{1+p_n(1-p_n)\left[\frac{\lambda^{(\aleph)}_\Delta}{2\alpha^{(\aleph)}\psi_{k\Delta,n}}\right]^2}, \end{aligned} \tag{59}$$

and the instantaneous conditional market price of risk for $\aleph$ is

$$\begin{aligned} \Phi\left(c^{(\aleph)}_{(k+1)\Delta,n} \mid \mathcal{F}^{(n,\aleph)}_k\right) &= \frac{E\left[c^{(\aleph)}_{(k+1)\Delta,n} \mid \mathcal{F}^{(n,\aleph)}_k\right] - \chi_{k\Delta,n}\Delta}{\sqrt{\mathrm{Var}\left[c^{(\aleph)}_{(k+1)\Delta,n} \mid \mathcal{F}^{(n,\aleph)}_k\right]\Delta}} \\ &= \frac{\varphi_{k\Delta,n} - \chi_{k\Delta,n} + \left(\lambda^{(\aleph)}_\Delta\right)^2 p_n(1-p_n)/(2\alpha^{(\aleph)})}{H(\aleph)\psi_{k\Delta,n}}. \end{aligned} \tag{60}$$

If $\aleph$ had not traded futures on the information possessed, the trader's instantaneous conditional market price of risk would have been the same as a noisy trader:

$$\Phi\left(c_{(k+1)\Delta,n} \mid \mathcal{F}^{(n)}_k\right) = \frac{E\left[c_{(k+1)\Delta,n} \mid \mathcal{F}^{(n)}_k\right] - \chi_{k\Delta,n}\Delta}{\sqrt{\mathrm{Var}\left[c_{(k+1)\Delta,n} \mid \mathcal{F}^{(n)}_k\right]\Delta}} = \frac{\varphi_{k\Delta,n} - \chi_{k\Delta,n}}{\psi_{k\Delta,n}}. \tag{61}$$

Thus, $\aleph's$ futures trading results in an (optimized) dividend $D^{\aleph}_{k\Delta}$ yield over the time interval $[k\Delta, (k+1)\Delta)$ determined by the solution of

$$\frac{\varphi_{k\Delta,n} + D^{\aleph}_{k\Delta} - \chi_{k\Delta,n}}{\psi_{k\Delta,n}} = \Phi\left(c^{(\aleph)}_{(k+1)\Delta,n}|\mathcal{F}^{(n,\aleph)}_k\right). \tag{62}$$

Thus,

$$D^{\aleph}_{k\Delta t} = (\varphi_{k\Delta,n} - \chi_{k\Delta,n})\left[\frac{1}{H(\aleph)} - 1\right] + \frac{p_n(1-p_n)\lambda^{(\aleph)^2}_\Delta}{2\alpha^{(\aleph)}H(\aleph)}. \tag{63}$$

We note that, relative to a noisy trader,

$$\mathrm{Var}\left[c^{(\aleph)}_{(k+1)\Delta,n} \mid \mathcal{F}^{(n,\aleph)}_k\right] = [H(\aleph)]^2\psi^2_{k\Delta,n}\Delta \geq \psi^2_{k\Delta,n}\Delta = \mathrm{Var}\left[c_{(k+1)\Delta,n} \mid \mathcal{F}^{(n)}_k\right]. \tag{64}$$

Equality between the first and last terms in (64) is obtained for $p_n = 0$ or $p_n = 1$ since, under these limits, all traders become aware of the direction of the price movement.

We investigate the dividend payout $D^{\aleph}_{k\Delta t}$ as a function of $\lambda^{(\aleph)}_\Delta$ and $\alpha^{(\aleph)}$. From (59) we note that $H(\aleph)$ is a monotonic function of $\lambda^{(\aleph)}_\Delta/\alpha^{(\aleph)}$ having the limits $H(\aleph) = 1$ and $H(\aleph) = \left[\sqrt{p_n(1-p_n)}/(2\psi_{k\Delta,n})\right](\lambda^{(\aleph)}_\Delta/\alpha^{(\aleph)})$. Under the limit $H(\aleph) = 1$, which corresponds to sufficiently small values of $\lambda^{(\aleph)}_\Delta$ or sufficiently large values of $\alpha^{(\aleph)}$,

$$D^{\aleph}_{k\Delta t} = \frac{p_n(1-p_n)\lambda^{(\aleph)^2}_\Delta}{2\alpha^{(\aleph)}}, \tag{65}$$

 doi:10.20944/preprints202502.0372.v1

which is always positive, increasing with $\lambda_\Delta^{(\aleph)}$ and decreasing as $\alpha^{(\aleph)}$ increases. Under the limit $H(\aleph) = \left[\sqrt{p_n(1-p_n)}/(2\psi_{k\Delta,n})\right](\lambda_\Delta^{(\aleph)}/\alpha^{(\aleph)})$, which corresponds to sufficiently large values of $\lambda_\Delta^{(\aleph)}$ or sufficiently small values of $\alpha^{(\aleph)}$,

$$\begin{aligned} D_{k\Delta t}^{\aleph} &= (\varphi_{k\Delta,n} - \chi_{k\Delta,n})\left[\frac{\alpha^{(\aleph)}}{\lambda_\Delta^{(\aleph)}}\frac{2\psi_{k\Delta,n}}{\sqrt{p_n(1-p_n)}} - 1\right] + \sqrt{p_n(1-p_n)}\lambda_\Delta^{(\aleph)}\psi_{k\Delta,n}. \\ &\approx \sqrt{p_n(1-p_n)}\lambda_\Delta^{(\aleph)}\psi_{k\Delta,n} - (\varphi_{k\Delta,n} - \chi_{k\Delta,n}). \end{aligned} \tag{66}$$

In this limit, the dividend payout is essentially independent of $\alpha^{(\aleph)}$.

7. Conclusion

Dynamic asset pricing based upon geometric Brownian motion (Black and Scholes 1973; Merton 1973) has had a tremendous' impact on finance theory. While having had difficulty gaining acceptance, dynamic pricing based upon arithmetic Brownian motion (Bachelier 1900) has certain attractive features. The unified BBSM model of Lindquist et al. (2024) encompasses the strengths of both models. By adapting the BBSM framework to a model of ESG-adjusted asset valuation, we put the full strength of the BBSM model to practical use. Using an empirical data set of 16 stocks taken from the Nasdaq-100, based on call option prices for 01/02/2024 we have shown that, generally, option traders were implying ESG-adjusted prices that exceed the spot price in the out-of-the-money region, while in-the-money, ESG-adjusted prices were lower that the spot price. A follow-up study is required to determine how universal an observation this may be. It would be interesting to investigate call option prices issued during periods of bull and bear markets, and during market disruptions.

We have further extended this ESG-BBSM model to consider futures trading strategy accessible to a trader $\aleph$ holding information on the direction of ESG-adjusted prices. It would be of interest to evaluate $\aleph$'s optimal dividend payout by, for example, projecting it forward on the binomial tree and computing an expected dividend at time $t+T$. While this could be evaluated for a specific asset, using historical estimated values $\hat{a}$, $\hat{\mu}$, $\hat{v}$, $\hat{\sigma}$, $\hat{\rho}$, $\hat{r}$, $\hat{Z}^{X;I}$, and a spot price S_t (with $\beta_t = S_t$), there is no historical information available for γ, while the parameters $\lambda_\Delta^{(\aleph)}$ and $\alpha^{(\aleph)}$ are trader-dependent. Thus, estimates of an expected average dividend payout at $t+T$ require an investigation of a three dimensional phase space - a fairly daunting prospect best left for a separate study.

Appendix H Tables

Table A1. Historical $[\gamma_l, \gamma_u]$ range and option price $\gamma^{(\mathrm{ESG,imp})}$ distribution summary statistics.

Ticker	$[\gamma_l, \gamma_u]$	Min	P_{25}	P_{50}	P_{75}	Max
AAPL	$[-1.16, 2.05]$	-1.02	-0.49	-0.16	-0.06	2.42
AMAT	$[-0.26, 0.32]$	-0.50	-0.23	-0.13	-0.03	0.58
AMD	$[-0.34, 0.46]$	-0.46	-0.32	-0.18	-0.10	1.03
AMZN	$[-0.36, 0.33]$	-1.04	-0.00	0.07	0.19	0.36
ASML	$[-1.03, 5.00]$	-0.35	-0.18	-0.08	-0.01	0.53
CSX	$[-0.43, 0.52]$	-0.45	-0.25	-0.09	0.10	0.60
DLTR	$[-0.37, 0.29]$	-0.79	-0.12	0.05	0.14	0.42
EA	$[-0.17, 0.15]$	-0.89	-0.27	-0.04	-0.01	0.24
GOOGL	$[-0.72, 0.63]$	-2.97	0.00	0.12	0.31	0.50
INTC	$[-0.13, 0.19]$	-0.30	0.00	0.11	0.49	1.45
NVDA	$[-0.42, 0.58]$	-0.36	-0.18	-0.08	-0.01	1.39
PANW	$[-0.09, 0.09]$	-1.36	-0.56	-0.25	-0.04	1.08
ROST	$[-0.33, 0.22]$	-0.18	0.02	0.04	0.11	0.26
TEAM	$[-0.78, 0.50]$	-1.94	-0.67	-0.12	0.08	0.25
WBD	$[-5.00, 1.04]$	-2.33	-1.06	-0.42	-0.08	0.30
WDAY	$[-0.55, 0.45]$	-0.66	-0.05	0.04	0.41	0.74

Preprints.org (www.preprints.org) | NOT PEER-REVIEWED | Posted: 6 February 2025 doi:10.20944/preprints202502.0372.v1

Table A2. Adjusted closing prices on 01/02/2024 for the 16 stocks studied.

AAPL	AMAT	AMD	AMZN	ASML	CSX	DLTR	EA
185.64	154.37	138.58	149.93	716.92	34.62	142.54	135.78
GOOGL	INTC	NVDA	PANW	ROST	TEAM	WBD	WDAY
138.17	47.80	481.68	288.92	137.68	226.67	11.66	268.28

Appendix I Plots of empirical option data $C^{(\mathrm{emp})}$

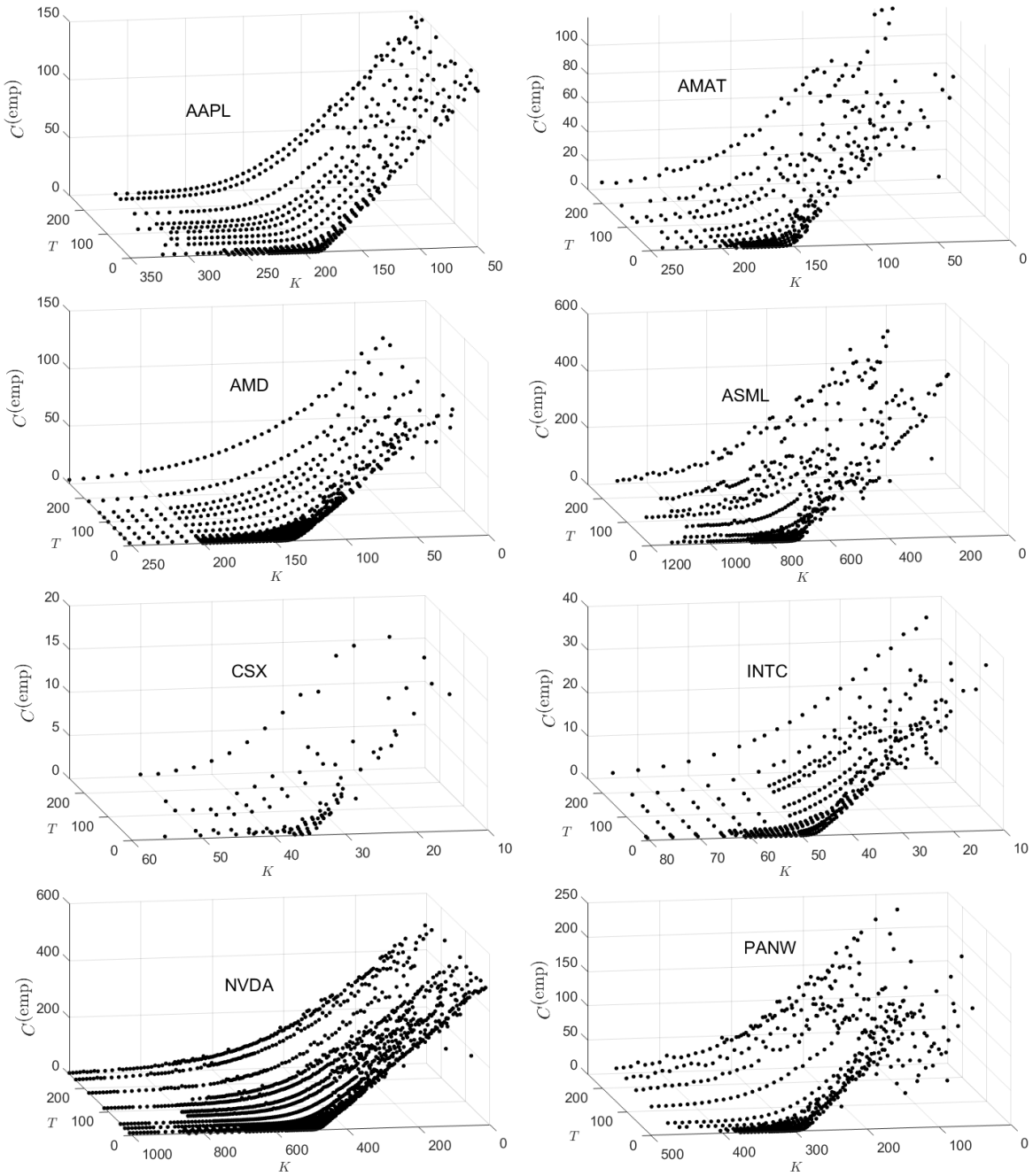

Figure B1 $C^{(\mathrm{emp})}$ for which $Z_t^{(X,)} > 0$ on $t = 01/02/2024$.

 doi:10.20944/preprints202502.0372.v1

Fig. B1 plots the empirical call option contract prices $C^{(\mathrm{emp})}$ as a function of strike price K and time to maturity T for the eight companies for which $Z_t^{(X,)} > 0$ for $t = 01/02/2024$ while Fig. B2 plots the same for the eight companies for which $Z_t^{(X,)} < 0$ for $t = 01/02/2024$

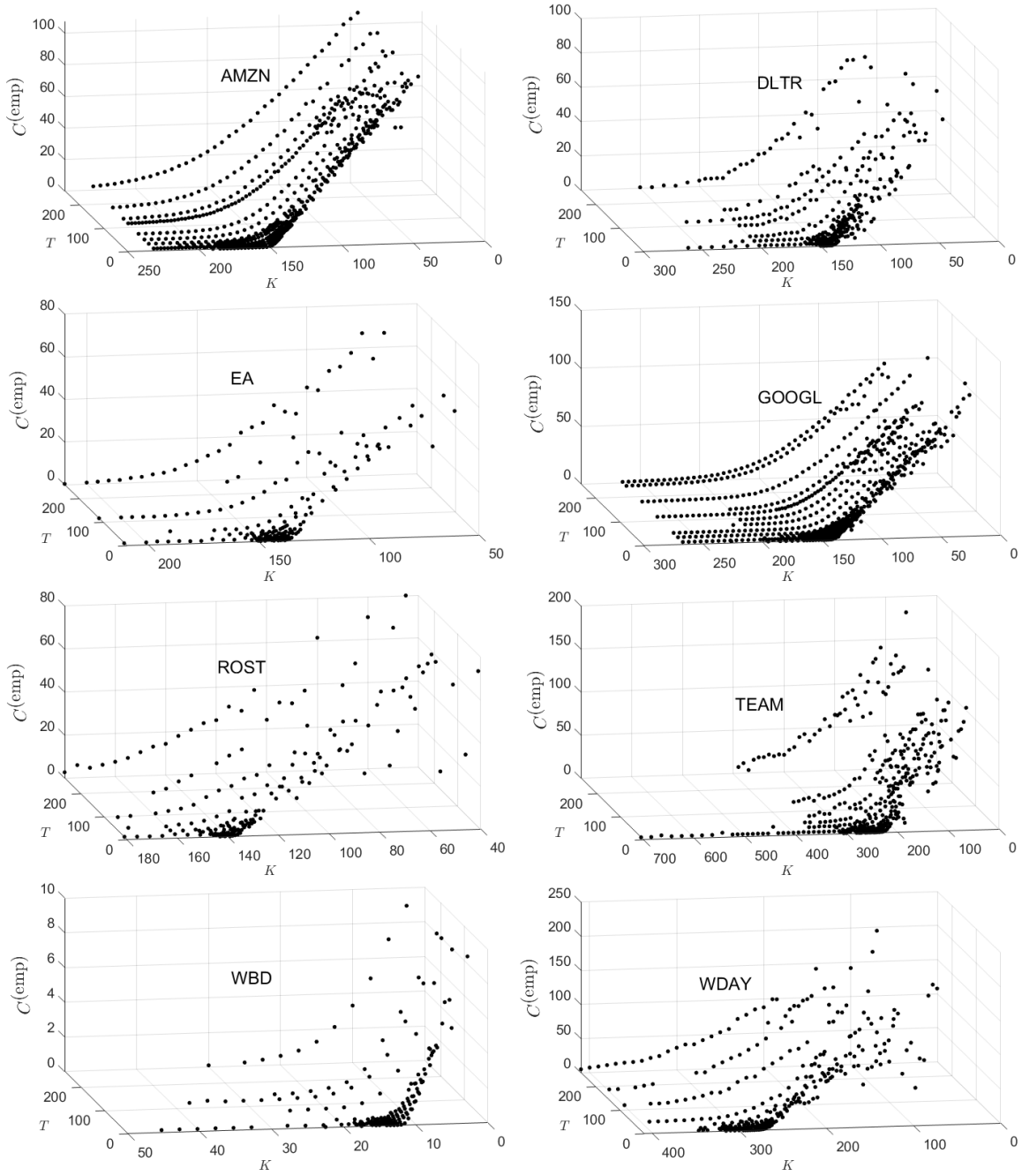

Figure B2 $C^{(\mathrm{emp})}$ for which $Z_t^{(X,)} < 0$ on $t = 01/02/2024$.

 doi:10.20944/preprints202502.0372.v1

Appendix J Plots of $\gamma^{(\mathrm{ESG,imp})}$

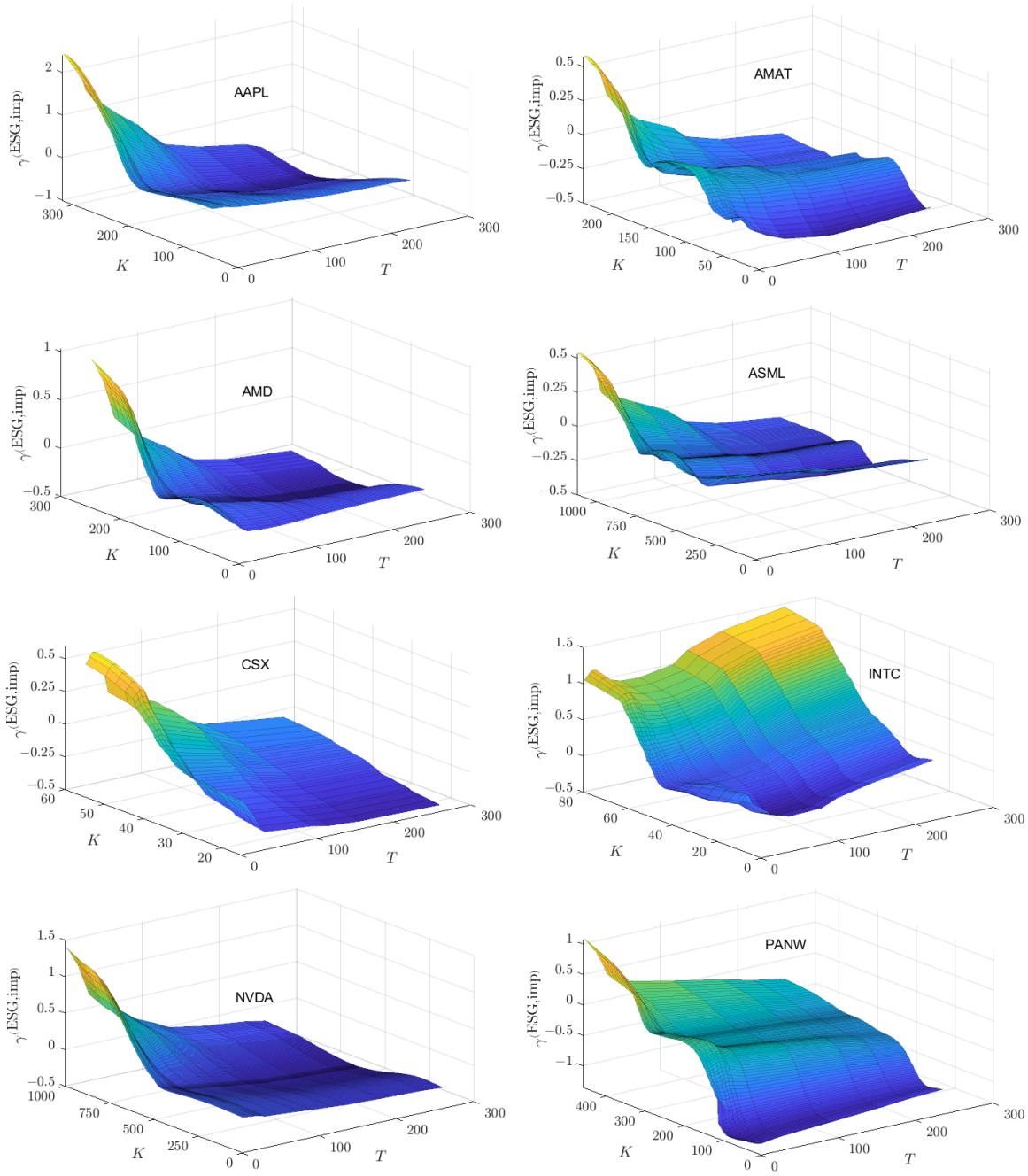

Figure C1 The implied surfaces $\gamma^{(,\mathrm{imp})}$ for which $Z_t^{(X,)} > 0$ on $t = 01/02/2024$.

Fig. C1 plots $\gamma^{(,\mathrm{imp})}$ as a function of strike price K and time to maturity T for the eight companies for which $Z_t^{(X,)} > 0$ on $t = 01/02/2024$.

 doi:10.20944/preprints202502.0372.v1

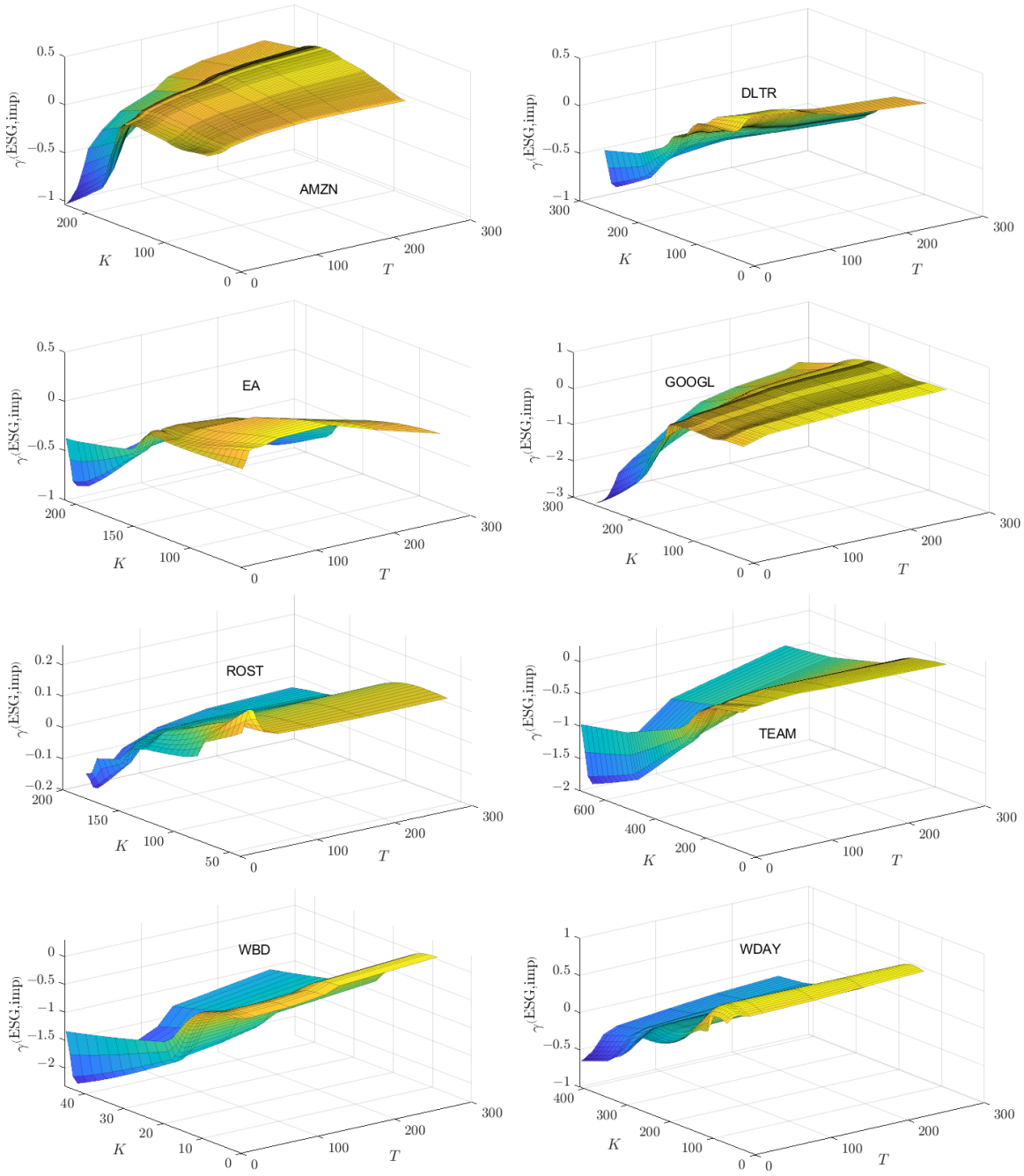

Figure C2 The implied surfaces $\gamma^{(,\mathrm{imp})}$ for which $Z_t^{(\mathrm{X},)} < 0$ on $t = 01/02/2024$.

Fig. C2 plots $\gamma^{(,\mathrm{imp})}$ for the eight companies for which $Z_t^{(\mathrm{X},)} < 0$ on $t = 01/02/2024$.

 doi:10.20944/preprints202502.0372.v1

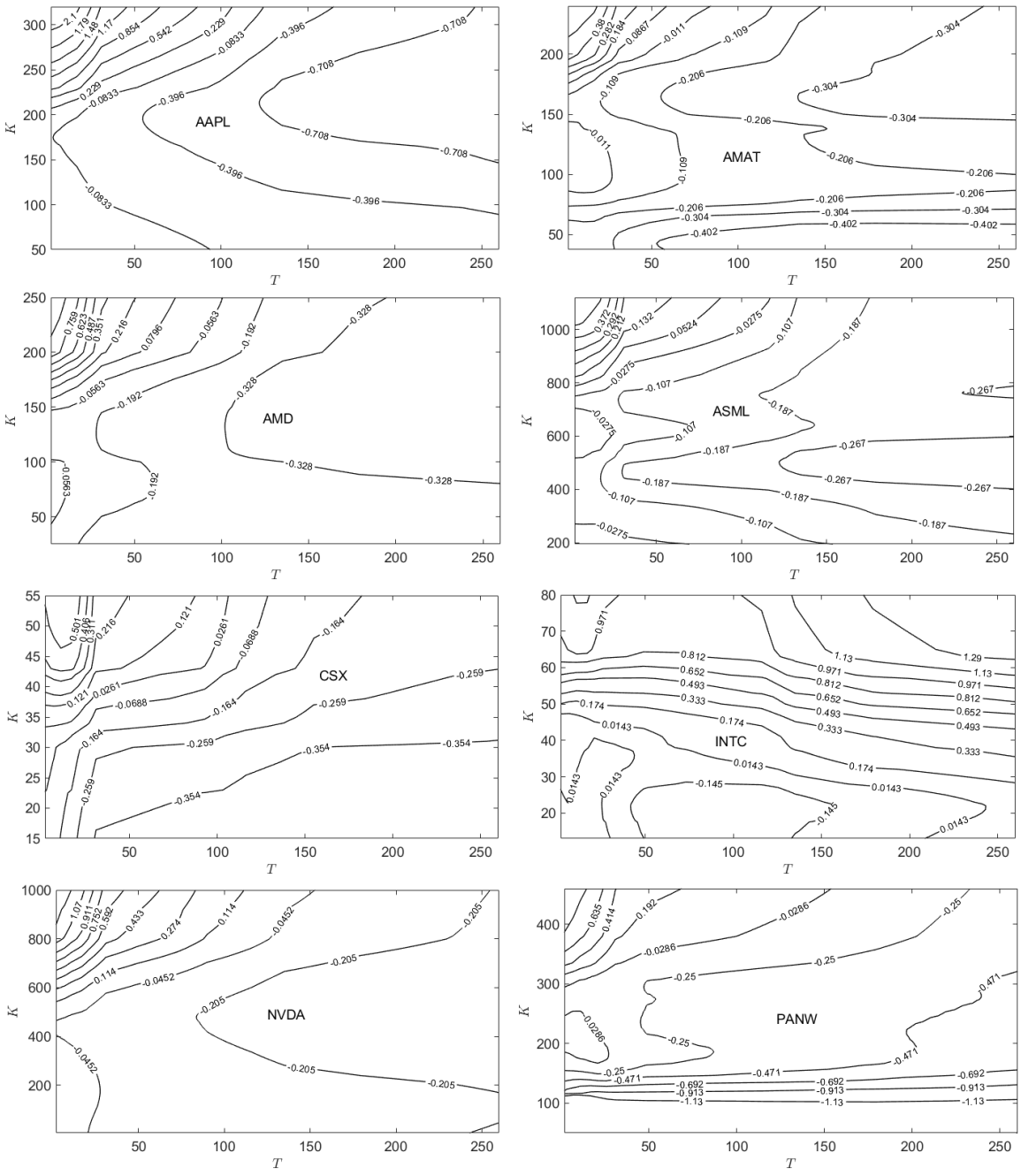

Figure C3 Contours of $\gamma^{(\mathrm{ESG,imp})}$ for which $Z_t^{(X;)} > 0$ on $t = 01/02/2024$.

Fig. C3 plots contours of $\gamma^{(\mathrm{ESG,imp})}$ as a function of strike price K and time to maturity T for the eight companies for which $Z_t^{(X,)} > 0$ for $t = 01/02/2024$, while Fig. C4 plots the same for the eight companies for which $Z_t^{(X,)} < 0$ for $t = 01/02/2024$

 doi:10.20944/preprints202502.0372.v1

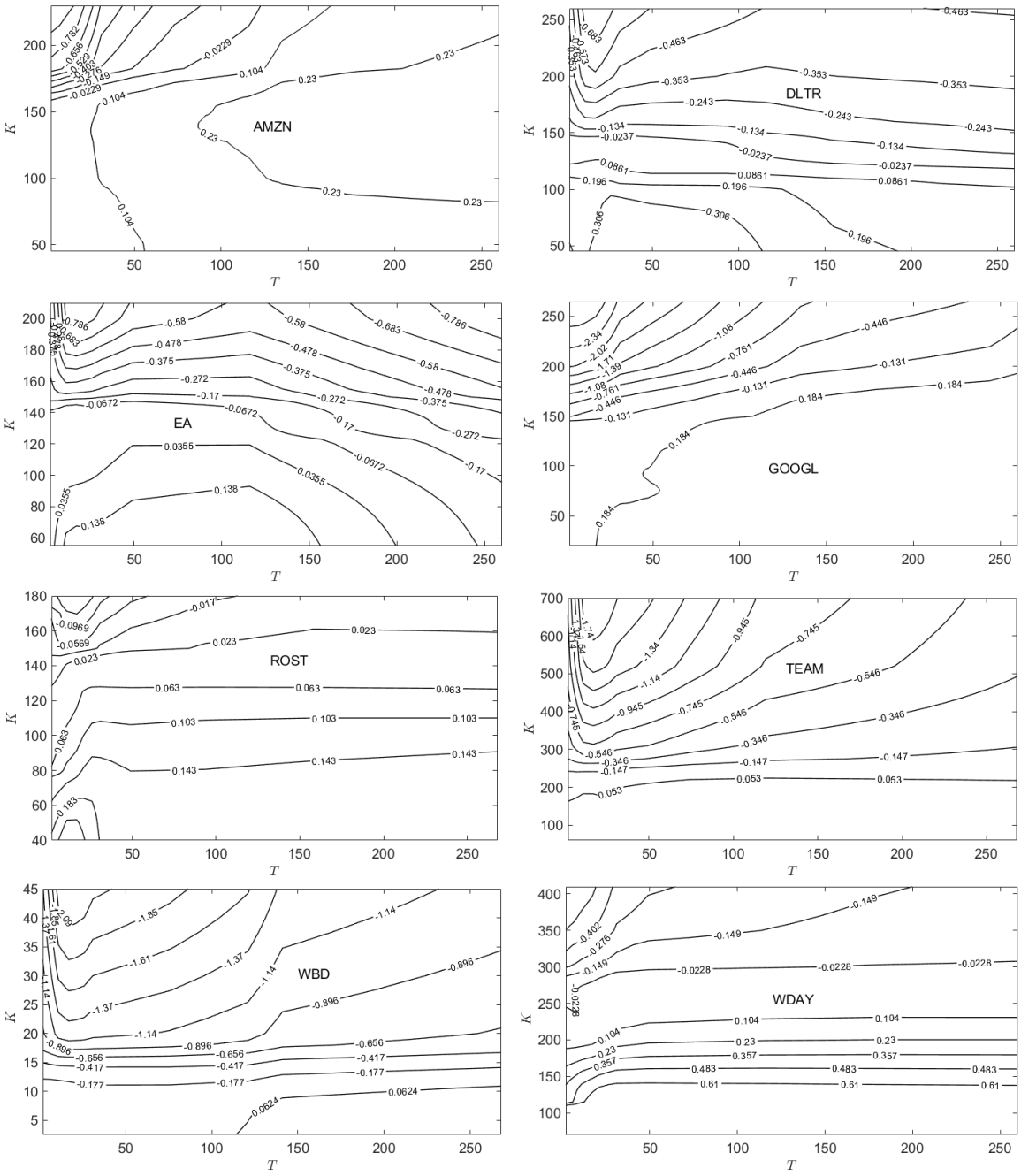

Figure C4 Contours of $\gamma^{(\mathrm{ESG,imp})}$ for which $Z_t^{(X,)} < 0$ on $t = 01/02/2024$.

 doi:10.20944/preprints202502.0372.v1

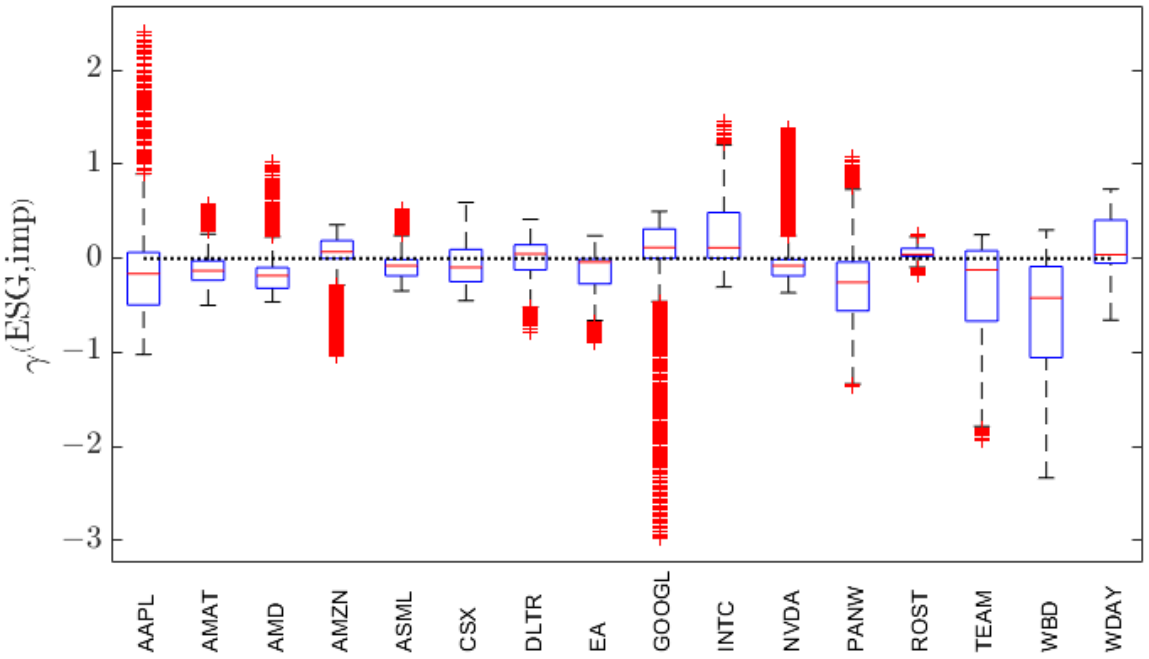

Figure C5 Box-whisker summaries of the distribution of $\gamma^{(\mathrm{ESG,imp})}$ values for all 16 stocks studied. The horizontal dotted-line indicates the value $\gamma^{(\mathrm{ESG,imp})} = 0$.

Fig. C5 presents the box-whisker summaries of the distributions of $\gamma^{(\mathrm{ESG,imp})}$ values for each of the 16 stocks.

 doi:10.20944/preprints202502.0372.v1

Appendix K Plots of $a_t^{(\mathbf{imp})}$

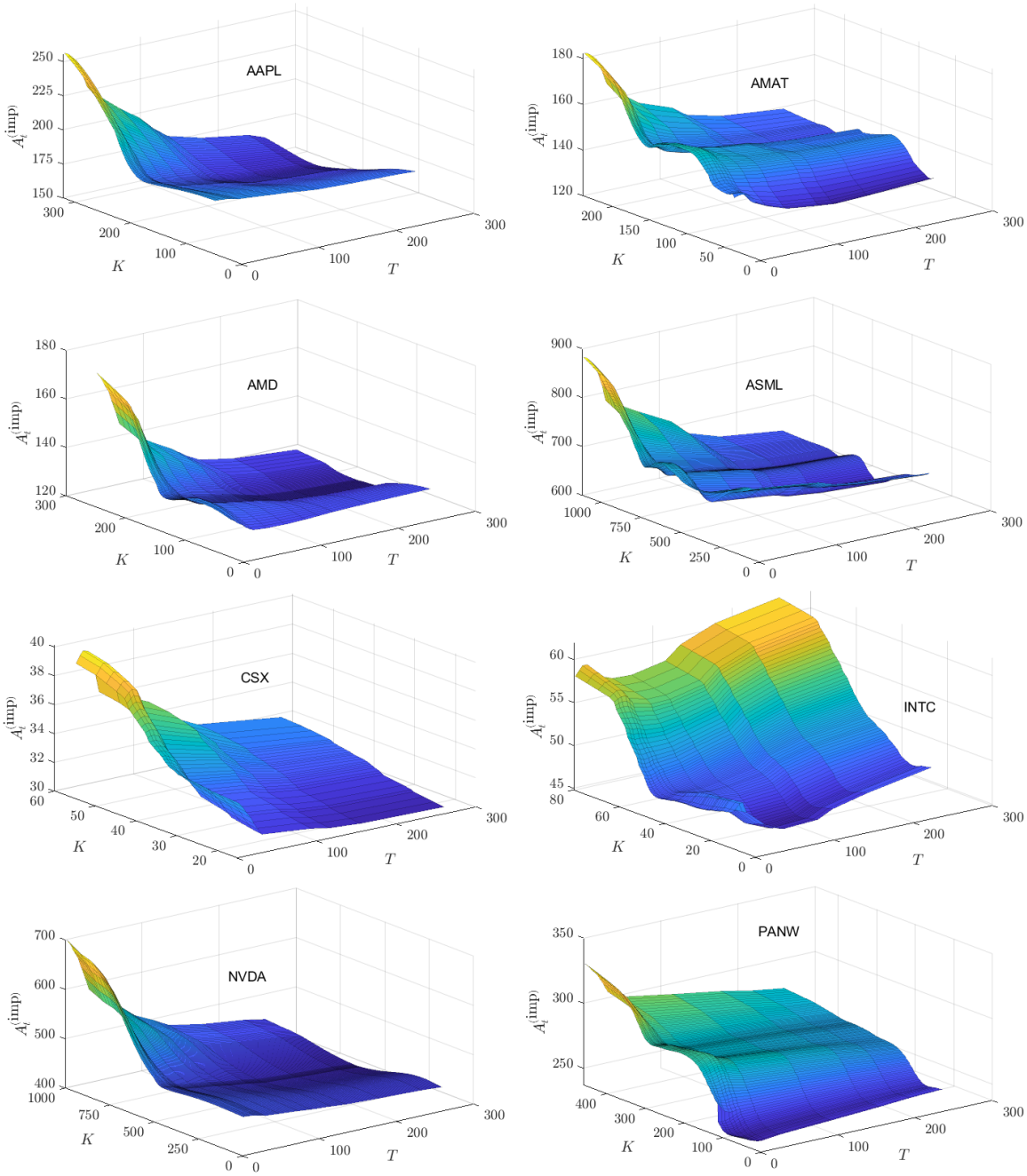

Figure D1 The surfaces $A_t^{(\mathrm{imp})}$ for which $Z_t^{(\mathrm{X},)} > 0$ on $t = 01/02/2024$.

Fig. D1 plots $A_t^{(\mathrm{imp})}$ as a function of strike price K and time to maturity T for the eight companies for which $Z_t^{(\mathrm{X},)} > 0$ for $t = 01/02/2024$, while Fig. D2 plots the same for the eight companies for which $Z_t^{(\mathrm{X},)} < 0$ for $t = 01/02/2024$

 doi:10.20944/preprints202502.0372.v1

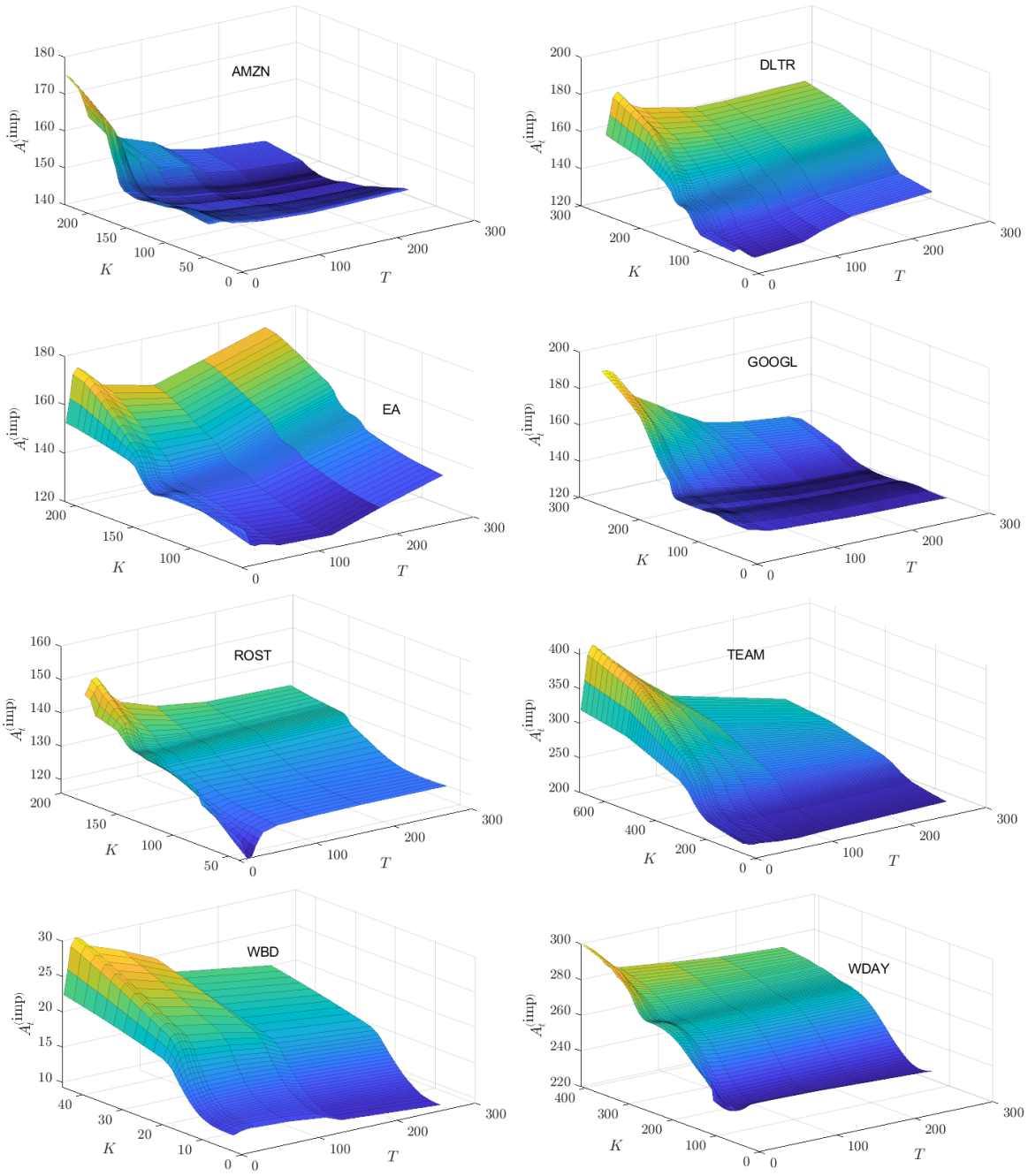

Figure D2 The surfaces $A_t^{(\mathrm{imp})}$ for which $Z_t^{(X,)} < 0$ on $t = 01/02/2024$.

 doi:10.20944/preprints202502.0372.v1

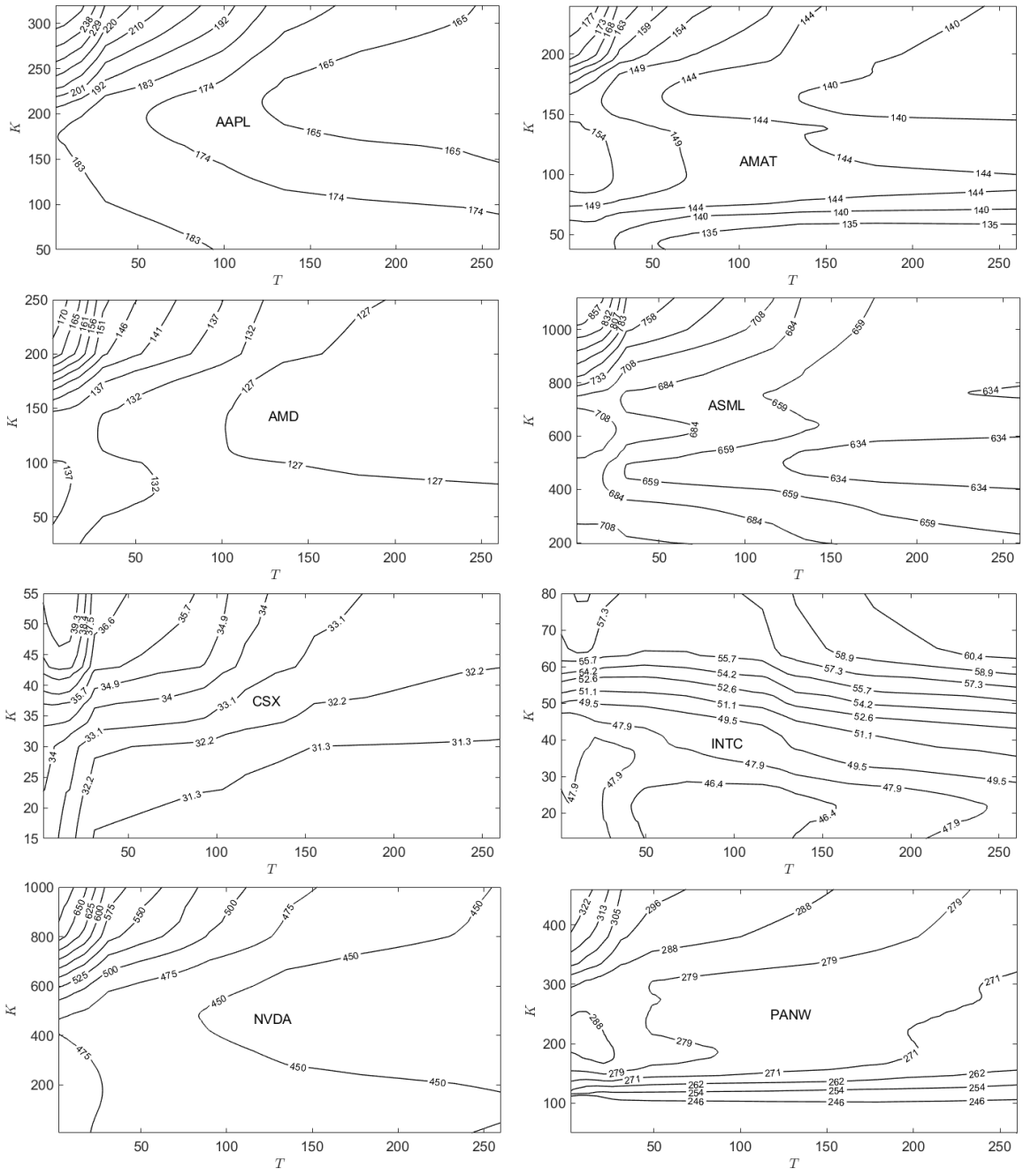

Figure D3 Contours of $A_t^{(\text{imp})}$ for which $Z_t^{(X,)} > 0$ on $t = 01/02/2024$.

Fig. D3 plots contours of $A_t^{(\text{imp})}$ as a function of strike price K and time to maturity T for the eight companies for which $Z_t^{(X,)} > 0$ for $t = 01/02/2024$ while Fig. D4 plots the same for the eight companies for which $Z_t^{(X,)} < 0$ for $t = 01/02/2024$

 doi:10.20944/preprints202502.0372.v1

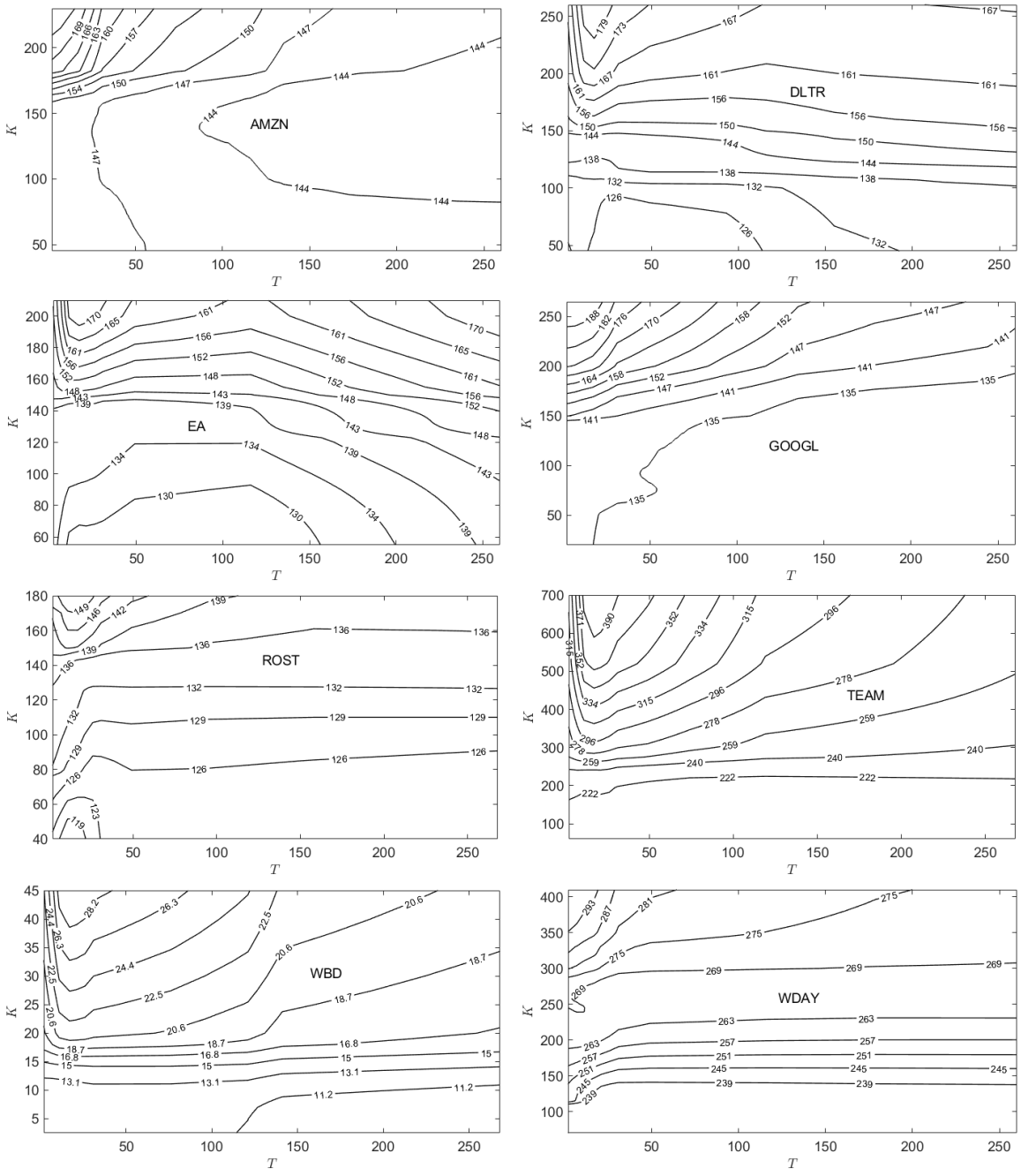

Figure D4 Contours of $A_t^{(\mathrm{imp})}$ for which $Z_t^{(X,)} < 0$ on $t = 01/02/2024$.

References

Abu-Mostafa, Yaser and Amir Atiya. 1996. Introduction to financial forecasting. *Applied Intelligence 6*, 205–213.

Alexander, Sidney S. 1961. Price movements in speculative markets: Trends or random walks. *Industrial Management Review 2*, 7–26.

Alexander, Sidney S. 1964. Price movements in speculative markets: Trends of random walks, Number 2. *Industrial Management Review 5*, 25–46.

Ang, Andrew, William Goetzmann, and Stephen Schaefer. 2010. The efficient market theory and evidence: Implications for active investment management. *Foundations and Trends in Finance 5*(3), 157–242.

Asare Nyarko, Nancy, Bhathiya Divelgama, Jagdish Gnawali, Blessing Omotade, Svetlozar T Rachev, and Peter Yegon. 2023. Exploring dynamic asset pricing within Bachelier's market model. *Journal of Risk and Financial Management 16*(8), 352.

Bachelier, Louis. 1900. Théorie de la spéculation. *Annales Scientifiques de l'Ecole Normale Supérieure 3*(17), 21–86.

 doi:10.20944/preprints202502.0372.v1

Black, Fischer and Myron Scholes. 1973. The pricing of options and corporate liabilities. *Journal of Political Economy 81*, 637–654.

Campbell, John and Samuel Thomson. 2008. Predicting the equity premium out of sample: Can anything beat the historical average? *The Review of Financial Studies 21*, 1509–1531.

Cervelló-Royo, Roberto, Francisco Guijarro, and Kristian Michniuk. 2015. Stock market trading rule based on pattern recognition and technical analysis: Forecasting the DJIA index with intraday data. *Expert Systems with Applications 42*, 5963–5975.

Chakravarty, Sugato, Huseyin Gulen, and Stewart Mayhew. 2004. Informed trading in stock and option markets. *The Journal of Finance 59*(3), 1235–1257.

Chong, Edwin, Han Chulwoo, and Colin Frank. 2017. Deep learning networks for stock market analysis and prediction: Methodology, data representations, and case studies. *Expert Systems with Applications 83*, 187–205.

Chung, Jaehun and Yongmiao Hong. 2014. Are the directions of stock price changes predictable? A generalized cross-spectral approach. In *Econometric Society 2004 North American Winter Meetings*. Econometric Society.

Collin-Dufresne, Pierre, Vyacheslav Fos, and Dmitry Muravyev. 2021. Informed trading in the stock market and option-price discovery. *Journal of Financial and Quantitative Analysis 56*(6), 1945–1984.

Cootner, Paul. 1964. *The Random Character of Stock Market Prices*. Cambridge, Massachusetts: M.I.T. Press.

Del Mar Miralles-Quiros, Maria, Jose Luis Miralles-Quiros, and Irene Guia Arraiano. 2017. Sustainable development, sustainability leadership and firm valuation: Differences across Europe. *Business Strategy and the Environment 26*(7), 1014–1028.

Duffie, Darrell. 2001. *Dynamic Asset Pricing Theory* (3rd ed.). Princeton, NJ: Princeton University Press.

Fama, Eugene. 1965. The behavior of stock market prices. *Journal of Business 38*, 34–105.

Fama, Eugene. 1970. Efficient capital markets: A review of theory and empirical work. *Journal of Finance 25*, 383–417.

Fama, Eugene. 1991. Efficient capital markets: II. *The Journal of Finance 46*, 1575–1617.

Fama, Eugene. 1995. Random walks in stock market prices. *Financial Analysts Journal 51*, 75–80.

Fulton, Mark, Bruce Kahn, and Camilla Sharples. 2012. Sustainable investing: Establishing long-term value and performance. Available at SSRN.

Hu, Yuan, Abootaleb Shirvani, Stoyan V Stoyanov, Young Shin Kim, Frank J Fabozzi, and Svetlozar T Rachev. 2020. Option pricing in markets with informed traders. *International Journal of Theoretical and Applied Finance 23*(06).

Jensen, Michael. 1978. Some anomalous evidence regarding market efficiency. *Journal of Financial Economics 6*(2/3), 95–101.

Leung, Mark, Hazem Daouk, and An-Sing Chen. 2000. Forecasting stock indices: A comparison of classification and level estimation models. *International Journal of Forecasting 16*, 173–190.

Lindquist, W Brent, Svetlozar T Rachev, Jagdish Gnawali, and Frank J Fabozzi. 2024. Dynamic asset pricing in a unified Bachelier–Black–Scholes–Merton model. *Risks 12*, 375.

Malkiel, Burton. 2003. The efficient market hypothesis and its critics. *Journal of Economic Perspectives 17*, 59–82.

Merton, Robert. 1973. Theory of rational option pricing. *Bell Journal of Economics and Management Science 4*, 141–183.

Naseer, Muhammad and Tehseen Yasir. 2014. The efficient market hypothesis: A critical review of the literature. *IUP Journal of Financial Risk Management 12*, 48–63.

Osborne, Michael. 1959. Brownian motion in the stock market. *Operations Research 7*, 145–173.

Qiu, Ming and Yu Song. 2016. Predicting the direction of stock market index movement using an optimized artificial neural network model. *PLoS ONE 11*(5), e0155133. https://doi.org/10.1371/journal.pone.0155133.

Rachev, Svetlozar T, Nancy Asare Nyarko, Blessing Omotade, and Peter Yegon. 2024. Bachelier's market model for ESG asset pricing. *Journal of Risk and Financial Management 17*(12), 553.

Rioul, Olivier. 2018. This is IT: A primer on Shannon's entropy and information. *L'Information, Séminaire Poincaré 23*, 43–77.

Robinson, David. 2008. Entropy and uncertainty. *Entropy 10*, 493–506.

Rubén, Alberto, Javier García, Francisco Guijarro, and Antonio Peris. 2017. A dynamic trading rule based on filtered flag pattern recognition for stock market price forecasting. *Expert Systems with Applications 81*, 177–192.

Shah, Dev, Haruna Isah, and Farhana Zulkernine. 2019. Stock market analysis: A review and taxonomy of prediction techniques. *International Journal of Financial Studies 7*, 26. https://doi.org/10.3390/ijfs7020026.

Shiller, Robert J. 2003. From efficient markets theory to behavioral finance. *Journal of Economic Perspectives 17*, 83–104.

 doi:10.20944/preprints202502.0372.v1

Turkington, Joshua and David Walsh. 2000. Informed traders and their market preference: Empirical evidence from prices and volumes of options and stock. *Pacific-Basin Finance Journal 8*(5), 559–585.

Zhong, Xiao and David Enke. 2017. Forecasting daily stock market return using dimensionality reduction. *Expert Systems with Applications 67*, 126–139.

Zhong, Xiao and David Enke. 2019. Predicting the daily return direction of the stock market using hybrid machine learning algorithms. *Financial Innovation 5*(1), 24. https://doi.org/10.1186/s40854-019-0138-0.